Communication Module
Mass Reduction

Forschungsgesellschaft Kraftfahrwesen mbH Aachen

Body Department

Final report

Communication Module
Mass Reduction

Project number

56690

Contractor:

International Iron and Steel Institute
WorldAutoSteel
Middletown, OHIO 45044-6211
USA

Project manager:

Project engineers:

Dipl.-Ing. Dipl.-Wirt. Ing. Roland Wohlecker
Group Leader Structural Analysis and Benchmarking

Dipl.-Ing. René Henn

Univ.-Prof. Dr.-Ing. Henning Wallentowitz
Head of ika

Dr.-Ing. Jörg Leyers
Managing Director fka

Aachen, November 2006

Contents

1   Introduction

Vehicles have historically been predominately made from conventional steel. Competition of OEMs and governmental demands for safer, lighter and more fuel economic cars led to the market entry of new materials such as new high-strength steels or aluminium. In this study especially the potential mass reduction impact of aluminium in comparison to conventional steels as well as to new steels is examined.

The main target of this study is, to visualise the weight difference between steel and aluminium and to communicate a feeling what a real weight difference can be. Especially the difference between recent and optimised steel design compared to aluminium is pointed out. So a perception of the differences between aluminium and steel concerning the mass potential of the body-in-white (BIW) is given. Therefore the following two often-stated as-sumptions are analysed:

1)   Vehicle mass can be reduced by 25 % through the application of modern high-strength and advanced high-strength steels [IIS06a] and

2)   vehicle mass can be reduced by up to 50 % by the application of aluminium [FUR03].

The base for these percentage comparisons is usually a 1990's-era former steel design. In this steel design very little high-strength or advanced high-strength steels were used. The other side of the spectrum for steel designs is the optimised steel design that contains up to 90 % high-strength (HHS) or ultra high-strength steels (UHSS). Today's vehicles are built in recent steel design that can be settled between the former and the optimised steel design.

Besides several vehicle body structures and components made of steel and aluminium are described and compared concerning their weight reduction potential. To compare mass in a neutral way, performance of the body structures and components must also be checked. But to establish fundamental reference points, a detailed description of material characteristics and basic structural behaviour for different materials are demonstrated first in this document.

To show the potential of aluminium and recent steel body structures, the body-in-white (BIW) of several vehicles is specified concerning body mass. To show the potential of optimised steels concept cars like the UltraLight Steel Auto Body, the Arcelor Body Concept and the ThyssenKrupp Steel NewSteelBody (NSB®) are summarised, showing mass reduction potential, performance and costs. Furthermore the weight development in the period of time between 1990 and 2005 is shown with the example of several vehicles.

Different components such as hoods, bumpers and front ends are compared concerning steel and aluminium applications based on similar performance. The analysis of hoods is based on studies by Forschungsgesellschaft Kraftfahrwesen mbH Aachen (fka) and the UltraLight Steel Auto Closures study for engine hoods. Also the bumper and front end chapters are based on fka studies.

2   Fundamentals

In an overview the significant definitions for the explanation of differences in steel and aluminium design are described. Therefore material characteristics and stiffness attributes as well as important terms are specified.

2.1   Material Characteristics

Steel offers a wide range of characteristics because of its numerous possibilities to influence the material properties during production and processing. Its characteristics can be influenced by the choice of the alloying constituents and the manufacturing parameters of the heat treatment and forming processes. Recently developed steel grades enable an increase in tensile strength and total elongation, so that the material can meet even higher requirements regarding the combination of strength and formability (Fig. 2-1). The shown steel grades are divided into three classes. Low strength steels are shown in dark grey, high-strength steels (HSS) in light grey and advanced high-strength steel (AHSS) are shown in colour. Stainless steel would be found in an area above that of conventional HSS and AHSS. It has a total elongation of approx. 45 to 55 % and a tensile strength of approx. 800 to 1500 MPa.

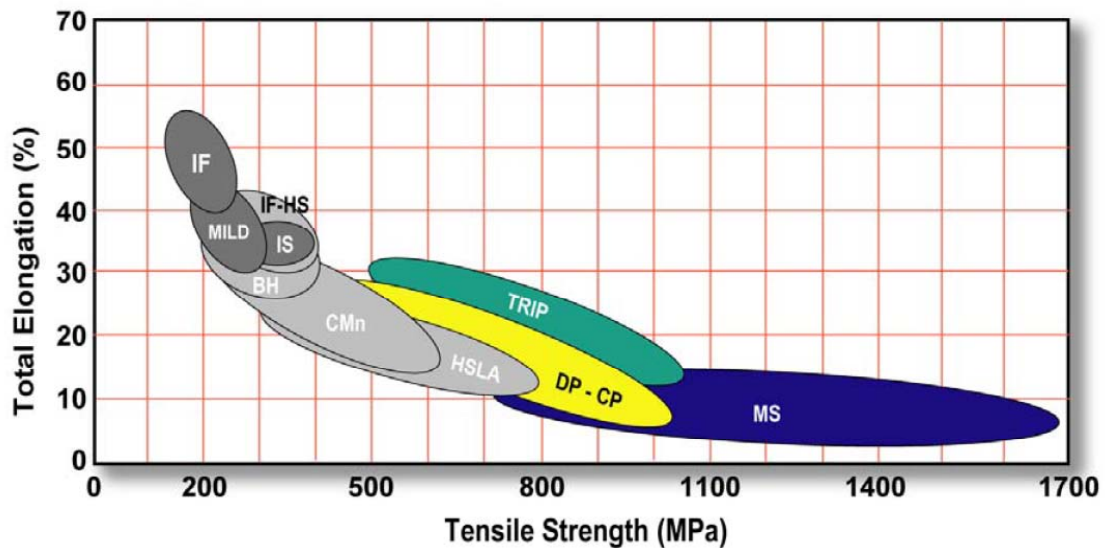Fig. 2-1:   Total elongation and tensile strength of different steel grades [IIS06b]

At the moment steel manufacturers are developing new steel grades called TWIP steel (Twinning Induced Plasticity). They have a total elongation of approx. 28 to 62 % and a tensile strength of approx. 800 to 1500 MPa [NIC05]. So in Fig. 2-1, they would be found in an area that lies even above that of stainless steel.

The range of aluminium does not cover such a large area in the elongation-strength diagram as steel does. The position of aluminium in comparison to steel is shown in Fig. 2-2. In this diagram also the area for hard aluminium alloys is given.
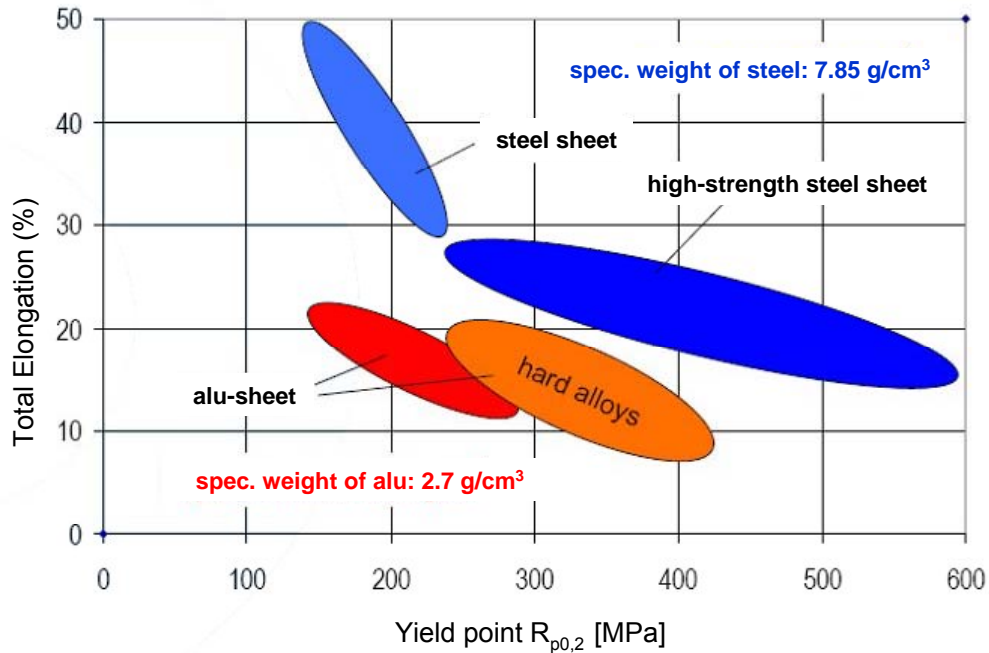
Fig. 2-2:   Total elongation and yield strength of aluminium [UFF06]

The current aluminium alloy development activities are mainly based on age hardening AlMgSi alloy systems. New aluminium alloys are developed and used with the aim to achieve a higher strength initial level as well as an improved age hardenability or to improve bending behaviour. Other alloys are used to improve crash performance [FUR05].

Further aluminium grades are developed with a tensile strength of 500 to 700 MPa. These high performance AlMgSc alloys are developed especially for future aircraft applications to compete with carbon fibre reinforced plastics [PAL06]. This shows what could be possible in future, but an application of these materials on the automotive sector is not planned, yet.

For outer panel applications aluminium alloy developments make it possible to obtain a higher dent resistance on the finished part after paint curing. This might lead to the use of thinner aluminium (down-gauging) and hence further weight reductions. The use of new aluminium alloys with optimal formability, allows higher complexity. So, while maintaining stiffness at a high level, the material thickness can be reduced, giving substantial cost savings [COR06].

2.2   General Structure and Mechanic Formulas

Fundamentals like bending and torsion stiffness as well as tensile strength are important in evaluation of vehicle body parts. Various fundamental parameters are proposed in literature

in order to compare the lightweight potential of different materials. An assortment of some important parameters for vehicle body structures are derived in this chapter. These parameters base on material-dependent parameters, like modulus of elasticity (E), density (ρ), tensile strength (R_m) and modulus of shearing (G), dedicated to the shape of typical body components. So, the parameters that are regarded for comparison of steel and aluminium in this chapter are:

- Bending stiffness parameter: $\dfrac{\sqrt[3]{E}}{\rho}$

- Tensile strength parameter: $\dfrac{R_m}{\rho}$

- Torsion stiffness parameter (open profile): $\dfrac{\sqrt[3]{G}}{\rho}$

- Torsion stiffness parameter (closed profile): $\dfrac{G}{\rho}$

- 3-point bending parameter: $\dfrac{R_m}{\rho}$

These parameters base on the assumption that the basic design of a component is independent of the material the part is made of. Specific advantages of alternative materials frequently turn out only after fundamental changes in the design of the component.

The different load cases on a vehicle body need some basic material properties, that are given in Fig. 2-3 for some steel grades as well as for some different aluminium materials. In this table the values for the modulus of elasticity (E), density (ρ), tensile strength (R_m) and the Poisson number (υ) are given for four steel grades (Mild 140/270, HSLA 350/450, DP 500/800 and MS 1250/1520) and for three aluminium materials (5457 O, 6060 T6 and 7021 T6). The modulus of shearing (G) can be calculated out of Eq. 2-1.

$$G = \frac{E}{2 \cdot (1+\upsilon)} \qquad\qquad\qquad \text{Eq. 2-1}$$

The influence of single load cases on vehicle body structures can be explained in simple beam examples at equal performance. One example is the load case bending stiffness that can be used for comparing the mass of steel and aluminium.

Material	Steel				Aluminium		
	Mild 140/270	HSLA 350/450	DP 500/800	MS 1250/1520	5457 O	6060 T6	7021 T6
Modulus of elasticity E [N/mm²]	210000	210000	210000	210000	72200	72200	72200
Tensile strength R_m [N/mm²]	270	450	800	1520	130	245	430
Density ρ [g/cm³]	7.85	7.85	7.85	7.85	2.7	2.7	2.7
Poisson number υ [1]	0.3	0.3	0.3	0.3	0.34	0.34	0.34
Modulus of shearing G [N/mm²]	81000	81000	81000	81000	26900	26900	26900

Fig. 2-3:   Material properties

2.2.1   Bending Stiffness

In Fig. 2-4 the load case for bending stiffness of a beam is regarded in detail. Examples for application of this load case in a body structure can be given, e.g. by a B-pillar or the rocker.
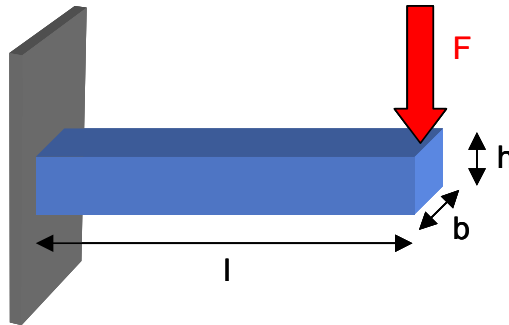

Fig. 2-4:   Load case for bending stiffness

As formulation for the load case bending stiffness at equal performance two fundamental formulas have to be used. The first equation is that for a bending line (Eq. 2-2).

$$\frac{F}{f} = \frac{3 \cdot I \cdot E}{l^3}$$

Eq. 2-2

To compare two materials at same performance the load (F) and the deflection (f) are constant.

$$\frac{F_1}{f_1} = \frac{F_2}{f_2}$$

Eq. 2-3

With Eq. 2-2 follows the equation for equal performance, that contains the modulus of elasticity (E) and the geometric moment of inertia (I). Because of the same conditions have to be considered here, the length (l) is set as constant.

$$E_1 \cdot I_1 = E_2 \cdot I_2$$

Eq. 2-4

The geometric moment of inertia for a rectangular profile is defined by Eq. 2-5.

$$I = \frac{b \cdot h^3}{12}$$

Eq. 2-5

The width (b) is also set as constant for both materials. So Eq. 2-4 turns into Eq. 2-6.

$$h_1^3 \cdot E_1 = h_2^3 \cdot E_2$$

Eq. 2-6

Converting this equation leads to Eq. 2-7.

$$\frac{h_1}{h_2} = \frac{\sqrt[3]{E_2}}{\sqrt[3]{E_1}}$$

Eq. 2-7

The mass is the product of density (ρ) and the volume (V) of the beam. The volume is the product of the three geometric parameters (l, b and h).

$$m = \rho \cdot l \cdot b \cdot h$$

Eq. 2-8

Comparing two beams at the same performance leads the term for the mass ratio:

$$\frac{m_1}{m_2} = \frac{l \cdot b \cdot \rho_1 \cdot h_1}{l \cdot b \cdot \rho_2 \cdot h_2}$$

Eq. 2-9

Because length and width are constant for both materials these variables can be released. Together with Eq. 2-7 this leads to:

$$\frac{m_1}{m_2} = \frac{\rho_1}{\rho_2} \cdot \sqrt[3]{\frac{E_2}{E_1}}$$

Eq. 2-10

This leads to the bending stiffness parameter: $\dfrac{\sqrt[3]{E}}{\rho}$

The material 2 is always the reference material Mild 140/270. So, if the mass ratio at equal bending stiffness (Fig. 2-5) reaches low values material 1 is lighter than Mild 140/270. Additionally the increase of height (h) resulting out of Eq. 2-7 is shown in this table. This height ratio is an indicator for the package demand of a material. The higher this value is the more package space needs the component to keep equal performance. So in this table that material has the most advantages that reaches the lowest values for the height ratio and the mass ratio at equal performance. This kind of description is used for all load cases that are studied in this chapter.

Material	Nomenclature	h_1/h_{ref}	m_1/m_{ref}
Steel	Mild 140/270 (reference)	1.0	1.0
	HSLA 350/450	1.0	1.0
	DP 500/800	1.0	1.0
	MS 1250/1520	1.0	1.0
Aluminium	5457 O	1.4	0.5
	6060 T6	1.4	0.5
	7021 T6	1.4	0.5

Fig. 2-5:   Height and mass ratio for bending stiffness parameter (dimensions not restricted)

The steel grades shown in the table have the same mass ratio as the mild steel and the same ratio of height. The mass ratio of the aluminium grades is with 0.5 lower and the height ratio is about 40 % higher. That means aluminium is in the load case bending stiffness at equal performance 50 % lighter, but it needs about 40 % more package space.

2.2.2   Tensile Strength

Another important parameter for body structures is the tensile strength (Fig. 2-6). Nearly every load on a component causes a tensile stress.
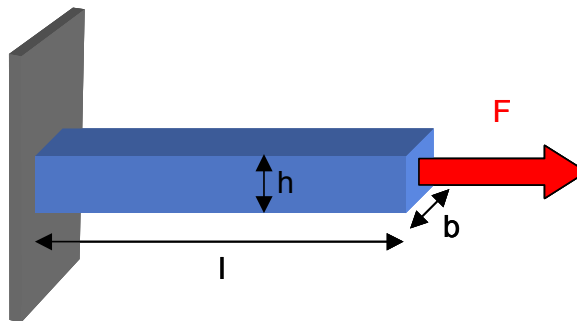

Fig. 2-6:   Load case for tensile strength

The formula for the longitudinal force in a beam contains the stress in the beam (σ) and the cross section surface (A).

$$F = \sigma \cdot A$$

Eq. 2-11

In this equation for the stress (σ) that is maximal possible the resistance to extension (R_m) is used. The cross section surface is the product of the width (b) and the height of the beam (h).

$$F_{max} = R_m \cdot h \cdot b$$

Eq. 2-12

As described in the derivation of bending stiffness the width shall be the same for both example beams (steel and aluminium). So the product of resistance to extension and height has to be constant, when both materials are compared.

$$R_{m1} \cdot h_1 = R_{m2} \cdot h_2$$

Eq. 2-13

A conversion of Eq. 2-13 leads to Eq. 2-14.

$$\frac{h_1}{h_2} = \frac{R_{m2}}{R_{m1}}$$

Eq. 2-14

Based on Eq. 2-8 the two materials can be compared for the same performance, now tensile strength, concerning their mass ratio.

$$\frac{m_1}{m_2} = \frac{l \cdot b \cdot \rho_1 \cdot h_1}{l \cdot b \cdot \rho_2 \cdot h_2}$$

Eq. 2-15

The two parameters for length and width are constant for both material examples again. In combination with Eq. 2-14 the two materials can be compared by tensile strength at same performance as given in Eq. 2-16.

$$\frac{m_1}{m_2} = \frac{\rho_1}{\rho_2} \cdot \frac{R_{m2}}{R_{m1}}$$

Eq. 2-16

This results in the tensile strength parameter: $\dfrac{R_m}{\rho}$

This factor should be as low as possible. Fig. 2-7 shows the results of the calculation used for the resistance to extension (R_m). Again material 2 is reference material Mild 140/270.

Material	Nomenclature	h_1/h_{ref}	m_1/m_{ref}
Steel	Mild 140/270 (reference)	1.0	1.0
	HSLA 350/450	0.6	0.6
	DP 500/800	0.3	0.3
	MS 1250/1520	0.2	0.2
Aluminium	5457 O	2.1	0.7
	6060 T6	1.1	0.4
	7021 T6	0.6	0.2

Fig. 2-7:   Height and mass ratio for tensile strength parameter (dimensions not restricted)

The lowest values for mass ratio at equal tensile strength are reached by MS 1250/1520. At the same time this material uses at least package space, because the lowest ratio of height can be reached. Aluminium 7021 T6 also reaches the mass ratio of MS1250/1520, but uses more package space. The mass ratio of DP500/800 can be found between the two aluminium grades 7021 T6 and 6060 T6 but also here, aluminium needs more package space. HSLA 350/450 has the same ratio of height like 7210 T6 and reaches the mass ratio of 5457 O, that has the highest demand for package space. So concerning equal tensile strength parameter MS1250/1520 and 7021 T6 reach the lowest mass ratio, both at the same level. At the same time aluminium needs more package space than steel grades with an equal mass ratio.

2.2.3   Torsion Stiffness

Besides the choice of material, the geometry of a component influences the mass depending weighting factors. These geometric influences are shown for the torsion stiffness of open and closed profiles.

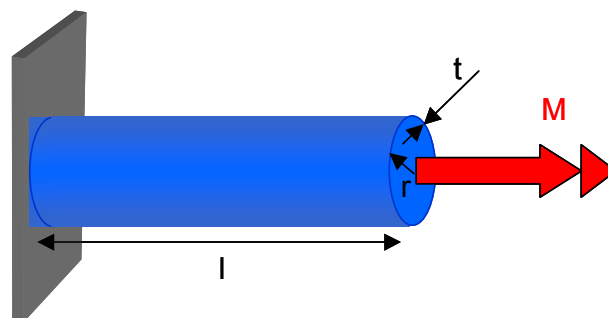
Fig. 2-8:   Load case for torsion stiffness (closed profile)

For an open round profile the torsion moment depends on the modulus of shearing (G), the polar moment of inertia (I_p), the length of the profile and the rotation angle (φ).

$$\frac{M_T}{\varphi} = \frac{G \cdot I_{P,O}}{l}$$

Eq. 2-17

The polar moment of inertia for a thin-walled opened round profile ($I_{p,o}$), shown in Eq. 2-18, contains the two geometric parameters radius (r) and thickness (t) [DIE92].

$$I_{P,O} = \frac{2 \cdot r \cdot \pi \cdot t^3}{3}$$

Eq. 2-18

Length and radius are constant for a steel profile as well as for an aluminium profile to reach the same package. So the term $G \cdot t^3$ has to be constant (Eq. 2-19) for the two regarded materials to reach the same performance.

$$G_1 \cdot t_1^3 = G_2 \cdot t_2^3$$

Eq. 2-19

This leads to the following ratio of thickness.

$$\frac{t_1}{t_2} = \frac{\sqrt[3]{G_2}}{\sqrt[3]{G_1}}$$

Eq. 2-20

Again the mass can be expressed as the product of volume and density (Eq. 2-8). So, the mass ratio for torsion of an open profile is given in Eq. 2-21.

$$\frac{m_1}{m_2} = \frac{2 \cdot \pi \cdot r \cdot l \cdot \rho_1 \cdot t_1}{2 \cdot \pi \cdot r \cdot l \cdot \rho_2 \cdot t_2}$$

Eq. 2-21

Because the radius (r) and the length (l) are constant this leads, including Eq. 2-20, to the relative mass for equal torsion stiffness:

$$\frac{m_1}{m_2} = \frac{\rho_1}{\rho_2} \cdot \frac{\sqrt[3]{G_2}}{\sqrt[3]{G_1}}$$

Eq. 2-22

So, the parameter of torsion stiffness for an open profile is: $\dfrac{\sqrt[3]{G}}{\rho}$

As before the mass ratio should reach low values. Fig. 2-9 shows that the mass ratio for aluminium is twice as low as that for the steel grades. In this table the package requirements are given by the thickness ratio because hollow profiles are used here. This thickness ratio is

about 40 % higher for aluminium. Once again material 2 is the reference material Mild 140/270.

Material	Nomenclature	t_1/t_{ref}	m_1/m_{ref}
Steel	Mild 140/270 (reference)	1.0	1.0
	HSLA 350/450	1.0	1.0
	DP 500/800	1.0	1.0
	MS 1250/1520	1.0	1.0
Aluminium	5457 O	1.4	0.5
	6060 T6	1.4	0.5
	7021 T6	1.4	0.5

Fig. 2-9:   Thickness and mass ratio for torsion stiffness parameter (open profile)

An equivalent formulation as for the open round profile is given in Eq. 2-23 for a closed round profile.

$$\frac{M_T}{\varphi} = \frac{G \cdot I_{P,C}}{l}$$
Eq. 2-23

Because the polar moment of inertia of a thin-walled closed round profile ($I_{p,c}$), shown in Eq. 2-24, differs from that of a thin-walled open round profile the result also differs.

$$I_{P,C} = 2 \cdot r^3 \cdot \pi \cdot t$$
Eq. 2-24

Within the fact that radius and length are constant for both materials to have the same package the term $G \cdot t$ has to be constant for aluminium and steel to reach the same performance.

$$G_1 \cdot t = G_2 \cdot t$$
Eq. 2-25

This leads to Eq. 2-26.

$$\frac{t_1}{t_2} = \frac{G_2}{G_1}$$
Eq. 2-26

As done before the materials are compared by mass ratio for equivalent performance:

$$\frac{m_1}{m_2} = \frac{2 \cdot \pi \cdot r \cdot l \cdot \rho_1 \cdot t_1}{2 \cdot \pi \cdot r \cdot l \cdot \rho_2 \cdot t_2}$$
Eq. 2-27

By attaching Eq. 2-26 and shortening the same variables like radius (r) and length (l) the term turns into Eq. 2-28. The reference material 2 is Mild 140/270 once again.

$$\frac{m_1}{m_2} = \frac{\rho_1}{\rho_2} \cdot \frac{G_2}{G_1}$$

Eq. 2-28

The resulting torsion stiffness parameter for a closed profile is: $\dfrac{G}{\rho}$

As a result (Fig. 2-10) the two factors for mass ratio at equal torsion stiffness for steel and aluminium reach the same value. This shows that in a closed profile, torsion stiffness does not depend on the material used. Due to that further designing issues like costs become more importance. Especially the package is very important at that point. The thickness ratio shows, that aluminium reaches three times higher package requirements than steel.

Material	Nomenclature	t_1/t_{ref}	m_1/m_{ref}
Steel	Mild 140/270 (reference)	1.0	1.0
	HSLA 350/450	1.0	1.0
	DP 500/800	1.0	1.0
	MS 1250/1520	1.0	1.0
Aluminium	5457 O	3.0	1.0
	6060 T6	3.0	1.0
	7021 T6	3.0	1.0

Fig. 2-10:   Thickness and mass ratio for torsion stiffness parameter (closed profile)

Without regarding the engaged material, it is better to use closed profiles for automotive tasks in principle. In these profiles the geometrical moment of inertia is exploited in a better way.

2.2.4   3-Point Bending

The last load case that has to be mentioned here is the 3-point-bending for a bending beam as shown in Fig. 2-11.

To describe this load case the formulation Eq. 2-29 can be used. The plastic load (F_{PL}) is given as a function of tensile strength (R_m), length (l), profile coefficient (α) and axial resistance moment (W_0).

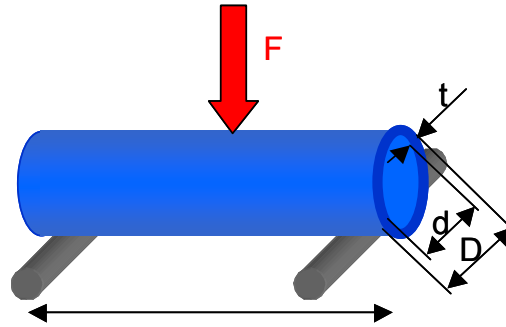$$F_{Pl} = \frac{4 \cdot \alpha}{l} \cdot R_m \cdot W_O$$

Eq. 2-29

6rh0098.doc

Fig. 2-11:   3-point-bending

The profile coefficient (α) can reach several values depending on the used profile. For a rectangle hollow profile it has a value of 1.0. A round hollow profile has a value of 1.5 and a round full section has a value of 1.7.

The axial resistance moment (W_0) contains the sheet thickness of the hollow profile (t) and the mean diameter of the profile (d_m). The mean diameter of the profile (d_m) in this term is the geometric middle of the outer diameter (D) and the inner diameter (d) of the hollow profile. The approach in the second part of the equation is based on the fact that the mean diameter of the profile (d_m) is much larger than the thickness of the hollow profile (t).

$$W_O = \frac{\pi \cdot \left(D^4 - d^4\right)}{32D} \approx \frac{\pi \cdot d_m^2 \cdot t}{4}$$

Eq. 2-30

For the formulation given in Eq. 2-29 this leads to the following term (Eq. 2-31).

$$F_{Pl} = \frac{\alpha \cdot d_m^2}{l} \cdot R_m \cdot t$$

Eq. 2-31

To compare two different materials at the same plastic load F_{PL} can be set constant for both materials. This results in Eq. 2-32.

$$R_{m1} \cdot t_1 = R_{m2} \cdot t_2$$

Eq. 2-32

This equation can be turned into Eq. 2-33.

$$\frac{t_1}{t_2} = \frac{R_{m2}}{R_{m1}}$$

Eq. 2-33

Once again the two materials are compared by mass ratio at equal performance.

$$\frac{m_1}{m_2} = \frac{\pi \cdot d_{m1} \cdot l \cdot \rho_1 \cdot t_1}{\pi \cdot d_{m2} \cdot l \cdot \rho_2 \cdot t_2}$$

Eq. 2-34

If the mean diameter of the profile (d_m) is much larger than the thickness of the hollow profile (t), the mean diameters for the two materials (d_{m1} and d_{m2}) are nearly equal.

$$\frac{m_1}{m_2} \approx \frac{\rho_1}{\rho_2} \cdot \frac{R_{m2}}{R_{m1}}$$ Eq. 2-35

From this follows the 3-point bending parameter: $\dfrac{R_m}{\rho}$

So the parameter for tensile strength and 3-point bending are equal if this approach is used. Like for the other load cases material 2 is Mild 140/270. This results in Fig. 2-12 that also reaches equal values as Fig. 2-7 with the same advantages for MS 1250/1520. Also on the package side the aluminium needs once again more package space than steel grade with equal mass ratio. The difference between 3-point bending and tensile strength is, that at tensile strengths the height ratio and for 3-point bending the thickness ratio is analysed.

Material	Nomenclature	t_1/t_{ref}	m_1/m_{ref}
Steel	Mild 140/270 (reference)	1.0	1.0
	HSLA 350/450	0.6	0.6
	DP 500/800	0.3	0.3
	MS 1250/1520	0.2	0.2
Aluminium	5457 O	2.1	0.7
	6060 T6	1.1	0.4
	7021 T6	0.6	0.2

Fig. 2-12:   Thickness and mass ratio for 3-point bending parameter

2.2.5   Conclusions

An overview of the described parameters is given in Fig. 2-13. This table shows, that especially regarding bending stiffness and torsion stiffness of an open profile aluminium requires 1.4 times more package space at the same performance. At the same time mass reduction by aluminium application reduces mass by 50 % in reference to a steel profile with equal performance. Regarding torsion stiffness of a closed aluminium profile, it needs a three times higher package space than a steel tube. Additionally the closed steel tube has the same weight as the aluminium tube.

Concerning tensile strength and 3-point bending, hot-rolled steel (e.g. MS 1250/1520) weighs as much as aluminium 7021 T6. Both materials are at equal performance 80 % lighter than a mild steel. A difference between hot-rolled steel and aluminium 7021 T6 can be found regarding the package. Steel requires 80 % less package than a mild steel and aluminium requires 40 % less package than a mild steel. Dual-phase steels (e.g. DP 500/800) reach in this two load cases a mass ratio that lies in the range of aluminium (7021 T6 and 6060 T6).

DP 500/800 is 70 % lighter than Mild 140/270 and aluminium 6060 T6 is 60 % lighter. At the same time the package demands of dual-phase steel is lower (60 % less than mild steel) than that of 6060 T6 (10 % more than mild steel). Also high-strength steel (e.g. HSLA 350/450) reaches a lower mass ratio than aluminium 5457 O and the same ratio of height as 7021 T6 at equal performance. The highest package demand in the two load cases tensile strength and 3-point bending can be found for aluminium 5457 O that needs 110 % more package space than mild steel, although it is 30 % lighter.

Material	h_1/h_{ref} resp. t_1/t_{ref}							m_1/m_{ref}						
	Steel				Aluminium			Steel				Aluminium		
Nomenclature	Mild 140/270 (reference)	HSLA 350/450	DP 500/800	MS 1250/1520	5457 O	6060 T6	7021 T6	Mild 140/270 (reference)	HSLA 350/450	DP 500/800	MS 1250/1520	5457 O	6060 T6	7021 T6
Bending stiffness	1.0	1.0	1.0	1.0	1.4	1.4	1.4	1.0	1.0	1.0	1.0	0.5	0.5	0.5
Tensile strength	1.0	0.6	0.3	0.2	2.1	1.1	0.6	1.0	0.6	0.3	0.2	0.7	0.4	0.2
Torsion stiffness (open)	1.0	1.0	1.0	1.0	1.4	1.4	1.4	1.0	1.0	1.0	1.0	0.5	0.5	0.5
Torsion stiffness (closed)	1.0	1.0	1.0	1.0	3.0	3.0	3.0	1.0	1.0	1.0	1.0	1.0	1.0	1.0
3-point bending	1.0	0.6	0.3	0.2	2.1	1.1	0.6	1.0	0.6	0.3	0.2	0.7	0.4	0.2

Fig. 2-13:   Summary of parameters

This shows that aluminium has a higher demand for package space than steel at equal performance. For the mass ratio the result depends on the regarded load case. Concerning bending and torsion stiffness, an open aluminium profile can be twice lighter than a steel profile. Regarding the other load cases steel and aluminium can be found in an equal mass range. In a real vehicle body these load cases are never seen for its own, always a combination of these load cases can be found.

2.3   Consequences for Real Body Components

Torsion and bending stiffness as well as tensile strength and 3-point bending are the most important load cases on vehicle body parts. These fundamental load cases result in stiffness and also strength parameters (see chapter 2.2), that allow to pre-select a material. More than that, these parameters belong to the basics of simulation software for crash simulation and topology optimisation in the vehicle development process and have a direct influence on the body design.

In addition to that this chapter shows the influence of a body part geometry on stiffness and mass. Also the utility of all described fundamentals regarding the performance and mass reduction potential of vehicle structures is displayed.

As shown in chapter 2.2 the different load cases cause different results for the mass ratio and the required package space. In most load cases aluminium requires more package than steel. This results in a bigger height or thicker profiles.

The cross section of a profile determines the mass as well as the thickness. The influence of these cross sections on the mass can be shown at the load cases for bending and torsion. Both load cases are divided in two package scenarios (Fig. 2-14).
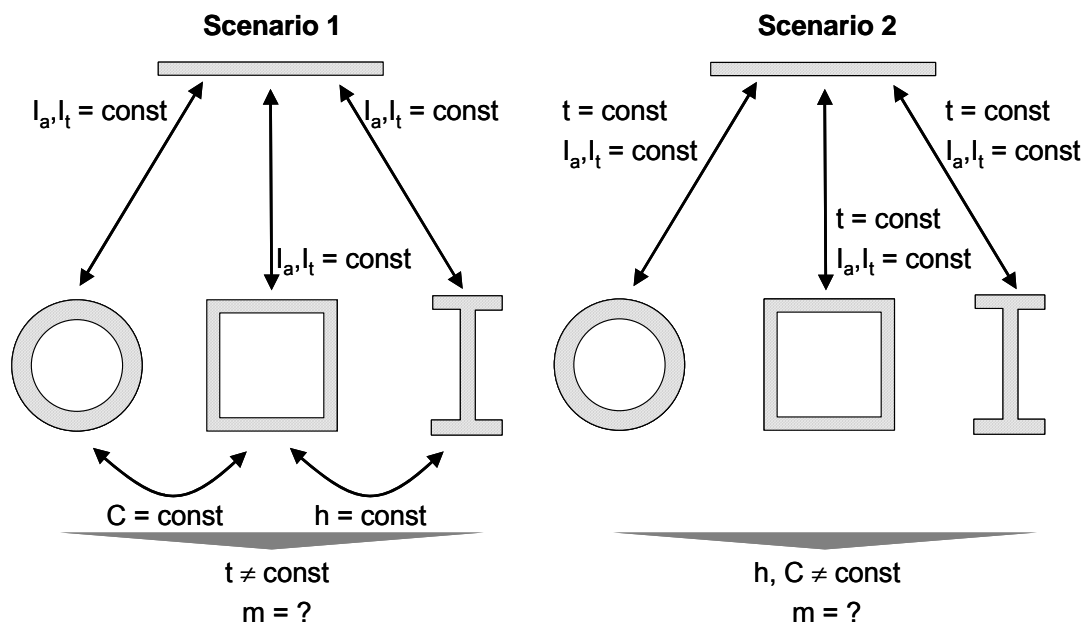

Fig. 2-14:   Correlation between cross sections for bending stiffness and torsion

In the first scenario the height of the profile is constant and a variation of the thickness of the profile is possible. In order to deal with comparable profiles the circumference (C) of the round tube and the rectangular hollow profile is set as equal. Besides, the double-T-profile and the rectangular hollow profile have the correlation of a constant height (h) in this scenario. The width (b) of the double-T-profile is set to the half value of the height (h).

In the second scenario the thickness is set to 2 mm as the constant parameter for both materials whereas the height or the circumference is variable. The correct choice of these variables has a big influence on the mass reduction potential. In addition for all profiles the axial (I_a) and also the torsional moment of of inertia (I_t) is set as constant, in order to provide always the same performance. When comparing steel with aluminium the modulus of elasticity (E) is considered in addition.

2.3.1   Influence of Cross Section at Bending Stiffness

In this chapter the influence of the profile geometry at the load case bending stiffness is regarded concerning the mass reduction potential. The equation for the mass is given in Eq. 2-8. It depends on the density of the used material, the cross section area and the length of the profile, that is set to l = 1000 mm. Therefore some different steel and aluminium profiles can be compared with a flat steel sheet as reference part.

The axial moment of inertia (I_a) is set to $I_a = 8000$ mm^4 for this load case. The formula for equal performance at bending stiffness is already given in Eq. 2-4 by E · I = const. So the axial moment of inertia (I_a) should be constant as shown in Eq. 2-36.

$$I_{a,1} = I_{a,2} \frac{E_2}{E_1}$$

Eq. 2-36

The comparison of steel profiles only shows, that the modulus of elasticity (E) is constant, so the ratio of E_2/E_1 is 1. But for the comparison of aluminium profiles with steel profiles E_2 is the modulus of elasticity for aluminium and E_1 is the modulus of elasticity for steel. Beneath the modulus of elasticity the axial moment of inertia is required for this comparison of aluminium and steel profiles. The cross section of a flat sheet is shown in Fig. 2-15.
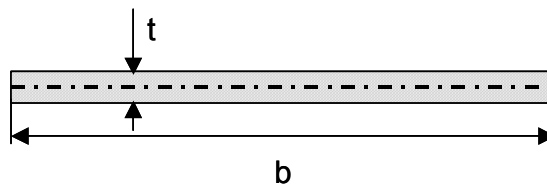

Fig. 2-15:   Cross section of flat sheet

The length (l) of all profiles is set to 1000 mm and the density (ρ) is given in Fig. 2-3. For the reference profile of a flat sheet the axial moment of inertia is shown in Eq. 2-37.

$$I_a = \frac{b \cdot t^3}{12}$$

Eq. 2-37

The mass of this profile results out of Eq. 2-8. Therefore the length, the density of the material and cross section area is needed. The cross section area depends on the width (b) and the thickness (t) as shown in Eq. 2-38.

$$A_{CS} = b \cdot t$$ Eq. 2-38

The first profile that is compared with this reference profile is a closed tube. The cross section of this profile is shown in Fig. 2-16.
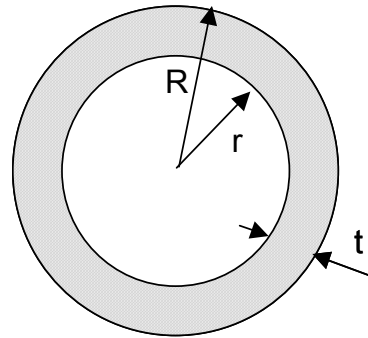

Fig. 2-16:   Cross section of a closed tube

The axial moment of inertia for this tube is shown in Eq. 2-39.

$$I_a = \frac{\pi}{4} \cdot \left(R^4 - r^4 \right)$$ Eq. 2-39

The cross section area of this profile follows out of Eq. 2-40.

$$A_{CS} = \pi \cdot \left(R^2 - r^2 \right)$$ Eq. 2-40

A rectangular hollow profile (Fig. 2-17) is analysed next. As an additional correlation the height (h) is equal to the width (b).

In the first scenario of constant height this profile should reach an equal circumfence as the closed tube. So the height (h) results in this scenario out of the comparison of the circumference of both profiles as given in Eq. 2-41.

$$2 \cdot R \cdot \pi = 4 \cdot h$$ Eq. 2-41

In the second scenario of constant thickness Eq. 2-41 is not necessary. The axial moment of inertia for the rectangular hollow profile has to reach the same performance for bending stiffness as that for the flat sheet in both scenarios. Therefore, in the second scenario the thickness is set to t = 2 mm and an adequate value for the height (h) has to be determined. The formula for the axial moment of inertia of this hollow profile results out of Eq. 2-42.

$$I_a = \frac{1}{12} \cdot \left(b \cdot h^3 - (b - 2 \cdot t) \cdot (h - 2 \cdot t)^3\right)$$ Eq. 2-42
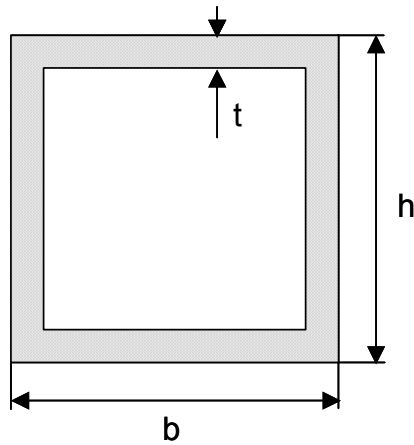
Fig. 2-17:   Cross section of a rectangular hollow profile

The cross section area of this profile is given by Eq. 2-43.

$$A_{CS} = b \cdot h - (b - 2 \cdot t) \cdot (h - 2 \cdot t)$$ Eq. 2-43

Further a double-T-profile is analysed in this context. The cross section of this profile is shown in Fig. 2-18. In the first scenario for constant height (h) the value for the height is equal to that of the rectangular hollow profile. The width (b) is half of the height (h).

Fig. 2-18:   Cross section of a double-T-profile

The axial moment of inertia of this profile is calculated by Eq. 2-44 and the cross section area by Eq. 2-45.

$$I_a = \frac{1}{12} \cdot \left(b \cdot h^3 - (b-t) \cdot (h - 2 \cdot t)^3 \right)$$

Eq. 2-44

$$A_{CS} = b \cdot h - (b-t) \cdot (h - 2 \cdot t)$$
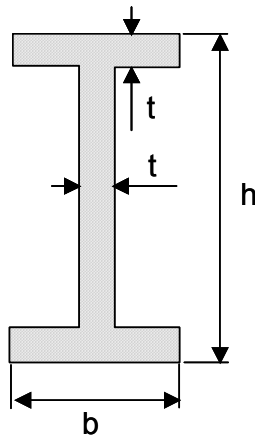
Eq. 2-45

The input parameters for a comparison of these profiles with the reference profile depends on the width (b), the height (h), the thickness (t) and the outer (R) and inner radius (r). Adequate parameters are evaluated by numerical calculations under consideration of the equations mentioned above. The target for all profiles is to achieve an axial moment of inertia of 8000 mm⁴.

The detailed values of these parameters for bending stiffness are given in Fig. 2-19 for the first scenario and in Fig. 2-20 for the second scenario. Out of these parameters result the cross section areas (A) and the masses (m) for the corresponding profiles (l = 1000 mm). Because of the simple geometry of the flat sheet the thickness (t) is equivalent to the height (h).

| Profile | Material | Scenario 1 (const. height) | | | | | | |
		b [mm]	h [mm]	t [mm]	R [mm]	r [mm]	A_{CS} [mm²]	m [kg]
flat sheet	steel	600.0	5.4		-	-	3257	25.41
	aluminium	600.0	7.7		-	-	4650	12.55
closed tube	steel	-	-	0.2	25.0	24.8	26	0.20
	aluminium	-	-	0.5	25.0	24.5	76	0.21
rectangular hollow profile	steel	39.3	39.3	0.2	-	-	31	0.25
	aluminium	39.3	39.3	0.6	-	-	93	0.25
double-T-profile	steel	19.6	39.3	0.4	-	-	32	0.25
	aluminium	19.6	39.3	1.3	-	-	97	0.26

constant performance: I_a =   8000   mm⁴

🟥 input parameter
🟩 intermediate results
🟨 results

Fig. 2-19:   Cross section parameters for bending stiffness (scenario 1)

These two tables show, that the closed tube and the rectangular hollow profile have a better bending stiffness than a flat sheet. An enormous decrease of the cross section area and the mass reduction is possible by these two profile types in comparison to a flat sheet. In the first scenario with a constant height the closed tube could reach the best results in this calculation. In the second scenario with a constant thickness the double-T-profile could reach the lowest mass and the lowest cross section area at the same time. So, this profile fits best to this load case.

6rh0098.doc

Profile	Material	Scenario 2 (const. thickness, t = 2 mm)						
		b [mm]	h [mm]	t [mm]	R [mm]	r [mm]	A_{CS} [mm^2]	m [kg]
flat sheet	steel	12000.0	2.0		-	-	24000	187.20
	aluminium	34903.0	2.0		-	-	69806	188.48
closed tube	steel	-	-	2.0	11.8	9.8	136	1.06
	aluminium	-	-	2.0	16.5	14.5	194	0.52
rectangular hollow profile	steel	20.1	20.1	2.0	-	-	145	1.13
	aluminium	27.9	27.9	2.0	-	-	207	0.56
double-T-profile	steel	12.4	24.8	2.0	-	-	91	0.71
	aluminium	17.3	34.6	2.0	-	-	131	0.35

constant performance: I_a =   8000   mm^4

🟥 input parameter
🟩 intermediate results
🟨 results

Fig. 2-20:   Cross section parameters for bending stiffness (scenario 2)

In a further overview the key results of steel vs. aluminium are shown (Fig. 2-21). The results of the first scenario can be summarised concerning the thickness ratio and the mass ratio of steel vs. aluminium. For the second scenario the ratio of height, the ratio of package area and the mass ratio are used for that comparison. All values are rounded.

Profile	Scenario 1		Scenario 2		
	t_{al}/t_{st}	m_{al}/m_{st}	h_{al}/h_{st}	$A_{P,al}/A_{P,st}$	m_{al}/m_{st}
flat sheet	1.4	0.5	3.0	3.0	1.0
closed tube	3.0	1.0	1.4	2.0	0.5
rectangular hollow profile	3.0	1.0	1.4	2.0	0.5
double-T-profile	3.0	1.0	1.4	2.0	0.5

Fig. 2-21: Summary of profile types for bending stiffness

The ratio of package area depends on the outer geometry of the profile. The package area characterises the space that is needed for the application of an profile. Because height is set constant in the first scenario for the closed tube, the rectangular hollow profile and the double-T-profile, this ratio has the value 1 in this scenario. So, the ratio of package is only important for the second scenario. For a flat sheet, a rectangular hollow profile and a double-T-profile the package area follows out of Eq. 2-46.

$$A_P = b \cdot h$$
Eq. 2-46

For the closed tube it follows out of Eq. 2-47.

$$A_P = \pi \cdot R^2$$
Eq. 2-47

6rh0098.doc

Fig. 2-21 shows, that similar to the results in Fig. 2-13 for the bending stiffness parameter, the flat sheet in scenario 1 and the three other profiles in scenario 2 reach a mass decrease of 50 % by the substitution of steel by aluminium. This goes along with a thickness or height increase of 40 %. In the second scenario this height increase leads to a two times higher package demand for aluminium profiles in comparison to steel profiles. On the other hand the flat sheet in scenario 2 and the three other profiles in scenario 1 have no mass decrease, but a three times higher thickness at the same mass level, when steel is substituted by aluminium. These results are similar to that for torsion stiffness of a closed profile in Fig. 2-13.

So, this analysis shows that the choice of the correct parameters for a vehicle body part are very important concerning bending stiffness. Both scenarios behave vice versa. Therefore it is very important if the height or the thickness of a body part will be changed. Aluminium profiles always have higher package demands than a steel profile. If the correct parameter is changed this will lead to a mass decrease in combination with a slight increase of thickness or height. But if the wrong geometric parameter is changed this substitution will not lead to a mass decrease in combination with a high increase of height and thickness. The double-T-profile behaves best at this load case. This means that a mass decrease is possible by the application of aluminium if the height of the body part can be changed. If this geometry should be unchanged aluminium has the same mass level as steel, but a three times higher thickness. If the package can be changed in height and the maximal possible weight reduction (50 %) should be realised, the package demand increases to a two times higher value. This shape is already shown in Fig. 2-13.

In the general case the structural package space is defined early in the design because of the needs to accommodate the passenger or defined by the packaging needs of other automotive components or ground clearance. So, in automotive design mostly the outer geometry (height or radius of a profile) is constant as realised in Scenario 1. With regard to this Scenario 1 represents the vast majority of design constraints for typical automotive structures. Scenario 2 is seldom the case due to package space restrictions.

2.3.2   Influence of Cross Section at Torsion Stiffness

The influence of the cross section for a 1000 mm long profile at torsion differs from that of bending. To reach the same performance G · I has to be constant (see chapter 2.2.3). So the torsional moment of inertia (I_t) is set constant by Eq. 2-48.

$$I_{t,1} = I_{t,2} \frac{G_2}{G_1}$$
                                                                                     Eq. 2-48

For the comparison of aluminium profiles with these steel profiles the reference profile is also a flat steel sheet. Because the modulus of shearing (G) of aluminium differs from that of steel the ratio of G_2/G_1 has to be considered. For the comparison of steel profiles this ratio has to be 1, because G is constant. In the comparison of aluminium profiles with steel profiles G_2 is

the modulus of shearing for aluminium and G_1 is the modulus of shearing for steel. For the reference part of a flat sheet (Fig. 2-22) the torsional moment of inertia is shown in Eq. 2-49. The correction factor (η_3) for a thin-walled sheet is 1 [DIE92].
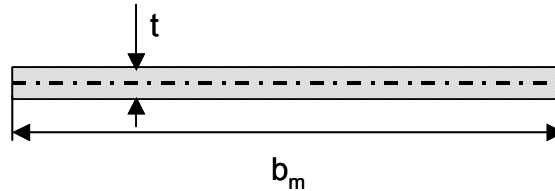

Fig. 2-22:   Cross section of flat sheet

$$I_t = \eta_3 \frac{b_m \cdot t^3}{3}$$

Eq. 2-49

The cross section area of this profile can be calculated by Eq. 2-50.

$$A_{CS} = b_m \cdot t$$

Eq. 2-50

To reach comparable cross sections, the thickness (t) and the width at the neutral axis (b_m) in the first scenario (constant height) are set to the corresponding value for the bending stiffness load case in that scenario. So the thickness is set to t = 5,429 mm and width to b_m = 600 mm in scenario 1. This results in a torsional moment of inertia of 32000 mm^4. All profiles for both scenarios have to reach this torsional moment of inertia in this load case. For the second scenario the thickness is set to a constant value of t = 2 mm for all profiles. So the width must be set to 12000 mm to reach this torsional moment of inertia.

The first profile that is compared with the flat sheet reference profile is a thin-walled closed tube. Its cross section is shown in Fig. 2-23.
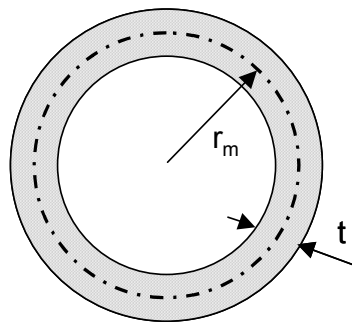

Fig. 2-23:   Cross section of a closed tube

The torsional moment of inertia for this profile is shown in Eq. 2-51 and the cross section area in Eq. 2-52.

$$I_t = 2 \cdot \pi \cdot t \cdot r_m{}^3$$

Eq. 2-51

$$A_{CS} = \pi \left(\left(r_m + \frac{t}{2} \right)^2 \cdot \left(r_m - \frac{t}{2} \right)^2 \right)$$

Eq. 2-52

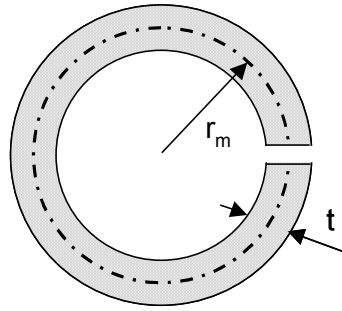In comparison to that the cross section of an open tube is pictured Fig. 2-24.

Fig. 2-24:   Cross section of an open tube

The torsional moment of inertia for this profile is shown in Eq. 2-53. It has nearly the same cross section area as the closed profile, that is why Eq. 2-52 is used for the cross section area.

$$I_t = \frac{2}{3} \cdot \pi \cdot t^3 \cdot r_m$$

Eq. 2-53

The next profile, that is analysed in this study, is a rectangular hollow profile shown in Fig. 2-25. In analogy to the load case for bending stiffness the package should be constant in the first scenario. Therefore, Eq. 2-41 is used once again to realise the correlation between a round and a rectangular profile in this scenario.
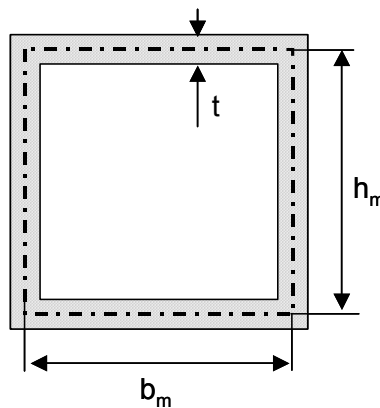
Fig. 2-25:   Cross section of a rectangular hollow profile

In the second scenario of constant thickness Eq. 2-41 is not used, because the thickness is set to $t = 2$ mm and an adequate value for the height of the neutral axis (h_m) has to be determined. The width of the neutral axis (b_m) is set to achieve the same value as the height h_m.

The torsional moment of inertia for this cross section is described in Eq. 2-54 [DIE92] and the cross section area in Eq. 2-55.

$$I_t = 2 \cdot t \cdot \frac{(b_m \cdot h_m)^2}{b_m + h_m}$$

Eq. 2-54

$$A_{CS} = \left(h_m + \frac{t}{2} \right) \cdot \left(b_m + \frac{t}{2} \right) - \left(h_m - \frac{t}{2} \right) \cdot \left(b_m - \frac{t}{2} \right)$$

Eq. 2-55

The last profile that is analysed here is the thin-walled double-T-profile (Fig. 2-26).
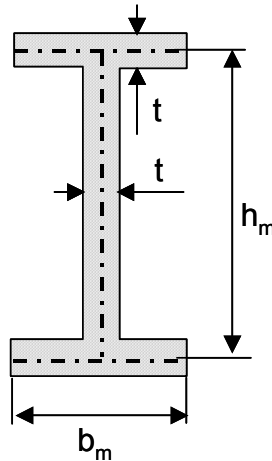
Fig. 2-26:   Cross section of a double-T-profile

The torsional moment of inertia is displayed in Eq. 2-56. The correction factor (η_3) for a thin-walled double-T-profile is set to $\eta_3 = 1.3$ [DIE92].

$$I_t = \frac{1}{3} \cdot \eta_3 \cdot (2 \cdot b_m + h_m) \cdot t^3$$

Eq. 2-56

The cross section area can be determined by Eq. 2-57.

$$A_{CS} = (h_m + t) \cdot b_m - (h_m - t) \cdot (b_m - t)$$

Eq. 2-57

Once again 1000 mm long profiles with these cross sections are analysed in the two scenarios for constant height and constant thickness. The input parameters for both scenarios are shown in Fig. 2-27 and Fig. 2-28. They depend on the width at the neutral axis

(b_m), the height at the neutral axis (h_m), the thickness (t) and the centre radius (r_m). These parameters have to reach the target value of 32000 mm^4 for the torsional moment of inertia of the steel reference.

| Profile | Material | Scenario 1 (const. height) | | | | | |
		b_m [mm]	h_m [mm]	t [mm]	r_m [mm]	A_{CS} [mm^2]	m [kg]
flat sheet	steel	600.0	5.4		-	3257	25.41
	aluminium	600.0	7.8		-	4704	12.70
closed tube	steel	-	-	0.3	25.0	51	0.40
	aluminium	-	-	1.0	25.0	154	0.52
open tube	steel	-	-	8.5	25.0	1333	10.40
	aluminium	-	-	12.3	25.0	207	5.20
rectangular hollow profile	steel	39.3	39.3	0.5	-	42	0.32
	aluminium	39.3	39.3	1.6	-	125	0.34
double-T-profile	steel	19.6	39.3	9.8	-	673	5.25
	aluminium	19.6	39.3	14.1	-	911	2.46

constant performance: I_t =   32000   mm^4

☐ input parameter
☐ intermediate results
☐ results

Fig. 2-27:   Cross section parameters for torsion stiffness (scenario 1)

| Profile | Material | Scenario 2 (const. thickness, t = 2 mm) | | | | | |
		b_m [mm]	h_m [mm]	t [mm]	r_m [mm]	A_{CS} [mm^2]	m [kg]
flat sheet	steel	12000.0	2.0		-	24000	187.20
	aluminium	36134.0	2.0		-	72268	195.12
closed tube	steel	-	-	2.0	13.7	172	1.34
	aluminium	-	-	2.0	19.7	248	0.67
open tube	steel	-	-	2.0	1909.9	24000	187.20
	aluminium	-	-	2.0	5750.9	72268	195.12
rectangular hollow profile	steel	25.2	25.2	2.0	-	101	0.79
	aluminium	36.4	36.4	2.0	-	146	0.39
double-T-profile	steel	2307.7	4615.4	2.0	-	18458	143.97
	aluminium	6948.8	13897.6	2.0	-	55587	150.08

constant performance: I_t =   32000   mm^4

☐ input parameter
☐ intermediate results
☐ results

Fig. 2-28:   Cross section parameters for torsion stiffness (scenario 2)

In both scenarios the flat sheet and the open tube reach the highest package demands and the highest mass values. Also the double-T-profile reaches high values for the cross section area and the mass. Therefore these three profiles are not well designed for a torsion load. Best values for mass reduction potential are reached by a closed tube and a rectangular hollow profile. In both scenarios the closed tube reaches the lowest mass level. Beyond, the rectangular hollow profile reaches the lowest cross section area values. So, concerning mass reduction potential the closed tube and the rectangular hollow profile show advantages in the torsion load case.

A comparison of steel vs. aluminium at equal torsion stiffness shows, that the two scenarios behave vice versa, once again. Once again steel is compared with aluminium by ratio of thickness and mass ratio in the two scenarios. In addition the ratio of package area is used in the second scenario.

As already described in chapter 2.3.1 it is necessary to show the ratio of package area for the second scenario. For a flat sheet, a rectangular hollow profile and a double-T-profile the package area follows out of Eq. 2-46 and for the closed and the open tube it follows out of Eq. 2-47.

Profile	Scenario 1		Scenario 2		
	t_{al}/t_{st}	m_{al}/m_{st}	h_{al}/h_{st}	$A_{P,al}/A_{P,st}$	m_{al}/m_{st}
flat sheet	1.4	0.5	3.0	3.0	1.0
closed tube	3.0	1.0	1.4	2.0	0.5
open tube	1.4	0.5	3.0	9.0	1.0
rectangular hollow profile	3.0	1.0	1.4	2.0	0.5
double-T-profile	1.4	0.5	3.0	9.0	1.0

Fig. 2-29:   Summary of profile types for torsion stiffness

In the first scenario a mass reduction of 50 % is possible by the application of aluminium of 50 % is possible in combination with a thickness increase of 40 % for the flat sheet, an open tube and double-T-profile. In the second scenario these profiles have no mass reduction potential when steel is substituted by aluminium and a three times higher ratio of mass. More than that the package demands of the open tube and the double-T-profile are more than nine times higher. But these profiles were identified as not adequate for this load case before.

The close tube and the rectangular hollow profile have in the first scenario no mass reduction potential at the comparison steel vs. aluminium and a three times higher thickness ratio. In the second scenario a mass reduction potential of 50 % and a height increase of 40 % is possible. This height increase leads to a two times higher package demand.

So for a closed tube and a rectangular hollow profile mass reduction by the application of aluminium is possible if the height can be changed and a two times higher package demand is acceptable. If this geometry should be unchanged aluminium has the same mass level as steel, but a three times thicker profile. This result is also shown in Fig. 2-13.

So for the bending load case the double-T-profile and for the torsional load case the closed tube as well as the rectangular hollow profile show the best performance. This explains how important the efficiency of a load path is. For bending beneath the double-T-profile, the closed tube and the rectangular hollow profile are the most efficient load paths. For torsion a closed tube or a rectangular hollow profile allow to realise the most efficient load paths. This shows that for torsion and bending the rectangular hollow profile is a good compromise. This is one reason why this kind of profile is often used for body parts.

As mentioned before Scenario 1 represents the vast majority of design constraints for typical automotive structures. Scenario 2 is seldom the case due to package space restrictions.

The closed sections result in the least mass solutions regardless of material selection resulting in mass reductions that are 1 and 2 orders of magnitude less than open profiles. These sections reduce the mass advantage of low density materials, when package space is tightly constrained such as it is in automotive structural applications.

2.3.3   Load Paths

Because in a vehicle body nearly all parts are influenced by more than one load case, the most used profile is a hollow profile. For the estimation of the material influence on bending stiffness and tensile strength in the chapters 2.2.1 and 2.2.2 a full-profile was used because its geometric moment of inertia is easier to handle and the profile stays constant in the comparison of the materials at one load case. But in a real vehicles these body parts are also hollow-profiles. In recent vehicles profiled body parts are made by shell-design or out of tubes. In the aluminium-space-frame design also extrusion profiles are used.

In addition to the thickness and the cross section geometry of a body the complexity of load is very important. The calculation of a load case that is combined by several different single load cases can get very complex. Simulation software in combination with FE-models helps to handle this problem and analyse e.g. the stiffness of a complete body structure. A high stiffness is necessary to improve driving performance as well as noise and vibrations damping. The numerical simulation allows to improve a vehicle's body structure with regard to stiffness. Therefore it is useful to analyse the structure for single load cases like bending and torsion first. In these simulations the fundamentals of chapter 2.2 are used.

Fig. 2-30 shows the deformation of a mini van structure under bending load. The forces (F_B) act symmetrically to the longitudinal axis of the vehicle. So, sufficient bending stiffness is provided mainly by its side structure. The intensive deflection of the doorsill and the longitudinal beams is easy to perceive.
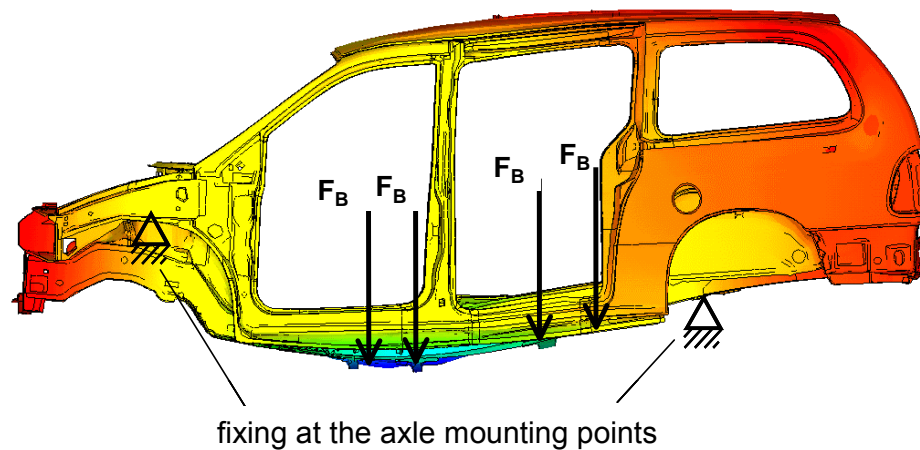
fixing at the axle mounting points

Fig. 2-30:   Bending behaviour of a vehicle body structure [WAL05]

Under torsion, both the side structure and the structural elements running in transversal direction are loaded. The magnified spatial deformation of a vehicle structure under torsion load is shown in Fig. 2-31. The torsion result out of the forces (F_T).
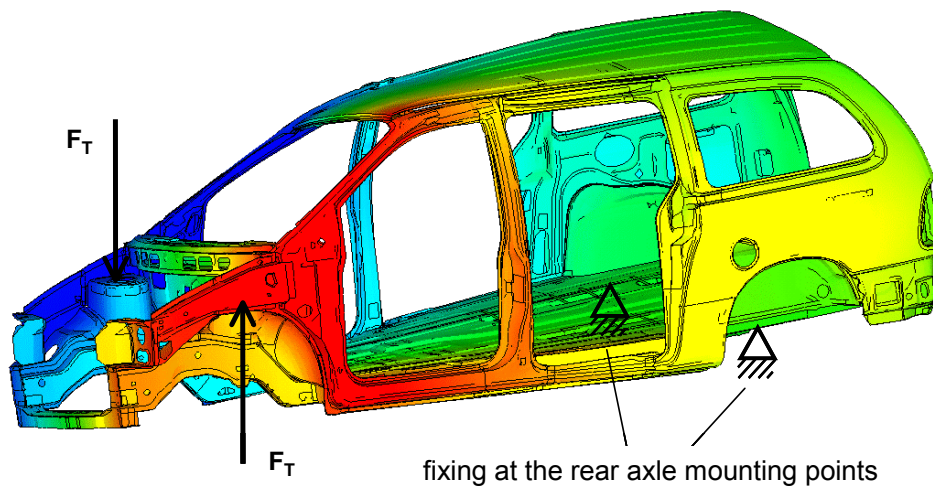

fixing at the rear axle mounting points

Fig. 2-31:   Torsion behaviour of a vehicle body structure [WAL05]

Not only in the numerical simulation, but also in physical tests, the body stiffness is assessed based on the deflection respectively distortion of the structure under static load. The vehicle can be supported at the axle mounting points and then loaded with defined weights to determine the deflection. The structural behaviour under torsion load can be tested by applying a torque to a beam, which is connected to the front axle mounting points by vertical rods and mounted on a pivot bearing. A test-bench for such tests is shown in Fig. 2-32.

torsional test   bending test
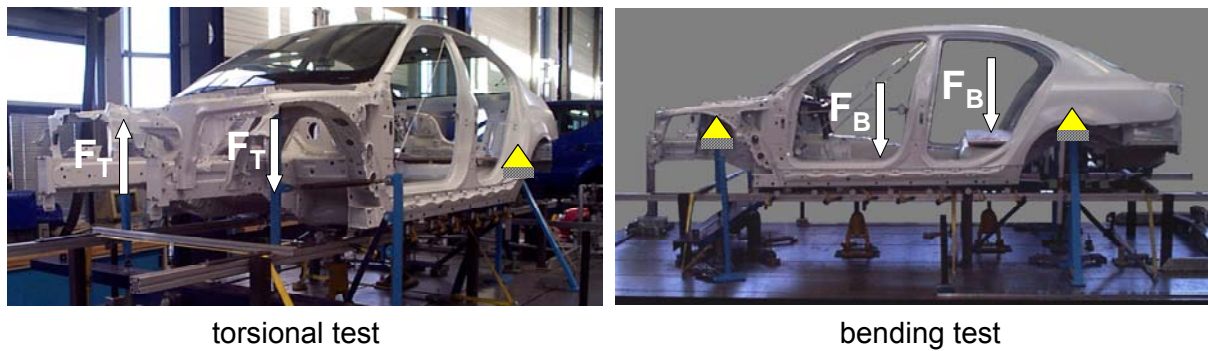
Fig. 2-32:   Measurement of body deformations under bending and torsion load [WAL05]

The detailed knowledge of static torsion and bending behaviour of the BIW can be used for improvements. By topology optimisation of the FE-model it is possible to find an optimised structure for bending and for torsion that fulfils the requirements of the single load cases in a better way. Fig. 2-33 shows the optimised structure for bending and torsion of a van. The different load paths can be identified clearly.

result of topology optimisation   result of topology optimisation
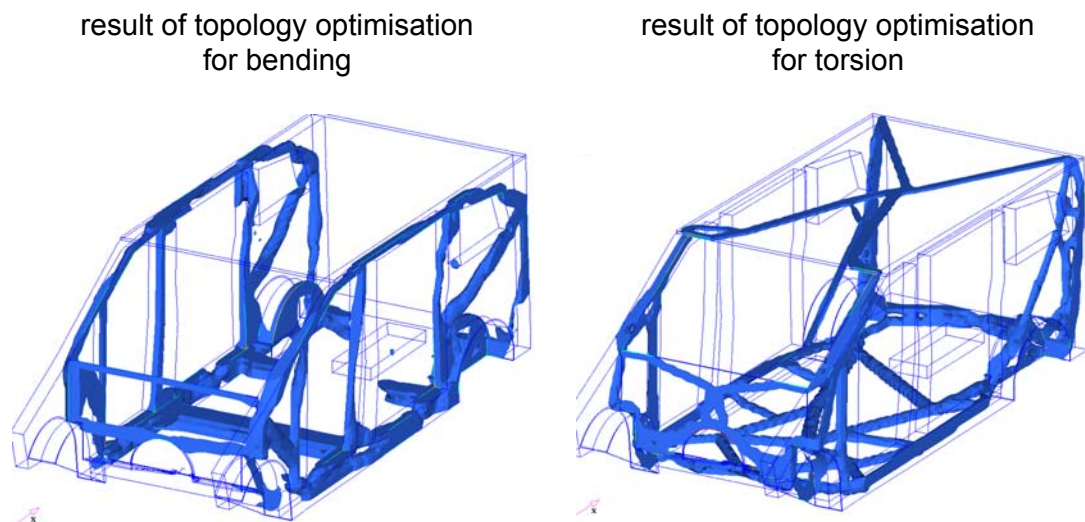for bending   for torsion

Fig. 2-33:   Results of topology optimisation for bending and torsion

Moreover real vehicles are loaded by torsion as well as by bending. These two load cases require different load paths that have to be considered in the body design and in the design of the body parts. At the same time the body weight should be minimised. The right compromise of these requirements can be evaluated out of a combined topology optimisation for both load cases. This results in an optimised body structure that fulfils both load cases. At the example of the van the optimised topology for a combination of bending and torsion is shown in Fig. 2-34.
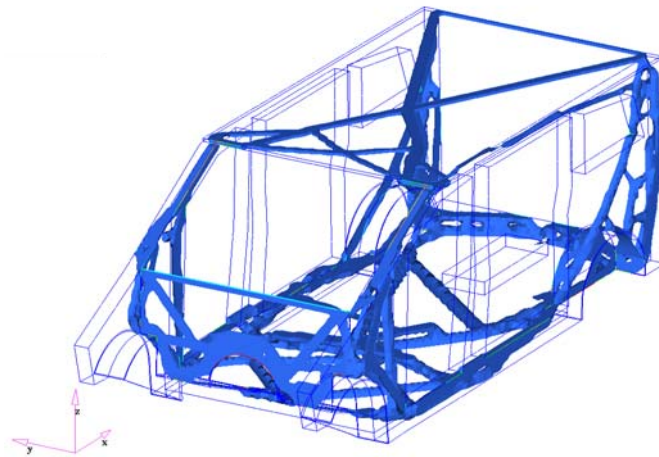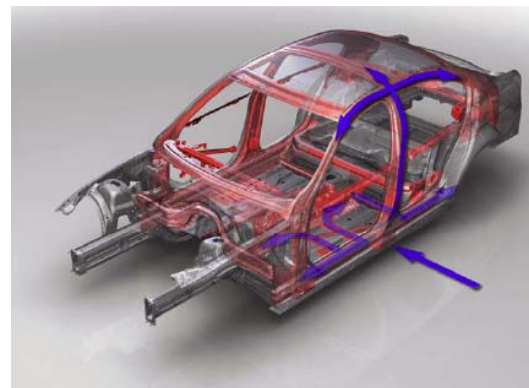
Fig. 2-34:   Results of topology optimisation for combination of bending and torsion

Another important point for body performance is the crash performance. Numerical crash calculation also bases on the fundamentals of chapter 2.2. Recent vehicles have to fulfil a crop of crash test (e.g. EuroNCAP, IIHS etc.). Two of the most important vehicle crash tests are the front and the side impact. Fig. 2-35 shows the different load paths of that two crash configurations.
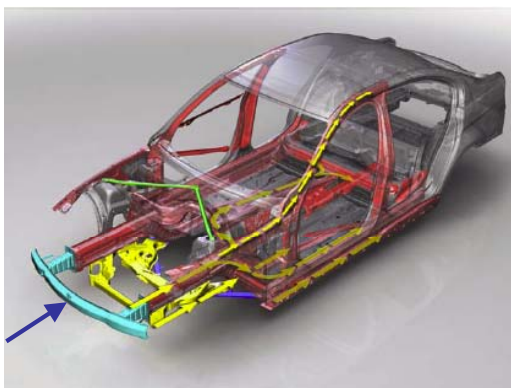
load path for front crash   load path for side crash

Fig. 2-35:   Load paths at front and side crash in the BMW 3-Series (E90) [AHL05]

The front crash load path starts at the bumper and proceeds via the longitudinal beams to the centre area of the vehicle. At a side impact the load path starts at the doorsill and the B-pillar and proceeds via the crossbeams in the floor and the roof area to the other side of the vehicle. So, in these two examples very different body components are a part of the load paths. This shows the complexity of the crash design for vehicle body structures.

The most important point in the development of a body structure is to find a suitable compromise between stiffness, crash performance and further body requirements (e.g. package etc.). In addition to the conflicting goals between these requirements, there are also

conflicts inside these requirements (e.g. different requirements of bending vs. torsion). To solve these problems is the main challenge in developing a body structure with the best possible performance and the lowest possible mass. Some solutions by OEMs and new concepts on that problem are described in chapter 3.

3   Selection of Adequate Components

In this chapter a detailed overview of mass and performance values of steel vs. aluminium based on existing and concept parts is given. The influence of material substitution in complete body structures are analysed as well as its influence on single vehicle sections, e.g. hoods or the front end.

3.1   Body Structures

The body structure of a vehicle shows very complex loading characteristics. To describe the possible load cases in a complete body structure all fundamentals of chapter 2.2 have to be applied. These fundamentals result in the potential for weight savings by usage of high-strength steels and alternative materials like aluminium in the body structure. Therefore series vehicles as well as concept cars are investigated in this chapter.

3.1.1   Body Structures of Series Vehicles

To show the mass reduction potential of vehicle bodies, several steel and aluminium series cars are described in detail concerning their body structures, body weight and production numbers.

3.1.1.1   Steel Body Structures

Nearly all OEMs apply steel as the body material. Fig. 3-1 shows the material spreading of the new BMW 3-Series E90 in comparison to the old model (E46) as an example. The E46 contains 55 % deep-drawn steel and 45 % AHSS. If in the body of the E90 the same materials have been used as in the E46, but the new model weigh 12 kg more [BRA05]. By application of multiphase-steel, which also belongs to the group of AHSS, a body weight of 267 kg (with closures) could be realised, which is 17 kg less than that of the previous model.

At the same time, torsion and bending stiffness were increased. Also crash performance has been improved, so that the new vehicle achieves five stars in the EuroNCAP crash test. This car reaches production numbers of approx. 500 000 per year.

A similar concept can be found in the new VW Passat that reaches production rates of approx. 520000 per year. Its body weight has been reduced in comparison to the previous model by 20 kg with identical layout criteria. The material spreading of this vehicle is shown in Fig. 3-2. At the same time torsion stiffness has been increased by 13 % and bending stiffness by 15 %. Although the crash performance and dimensions increased [STA05].
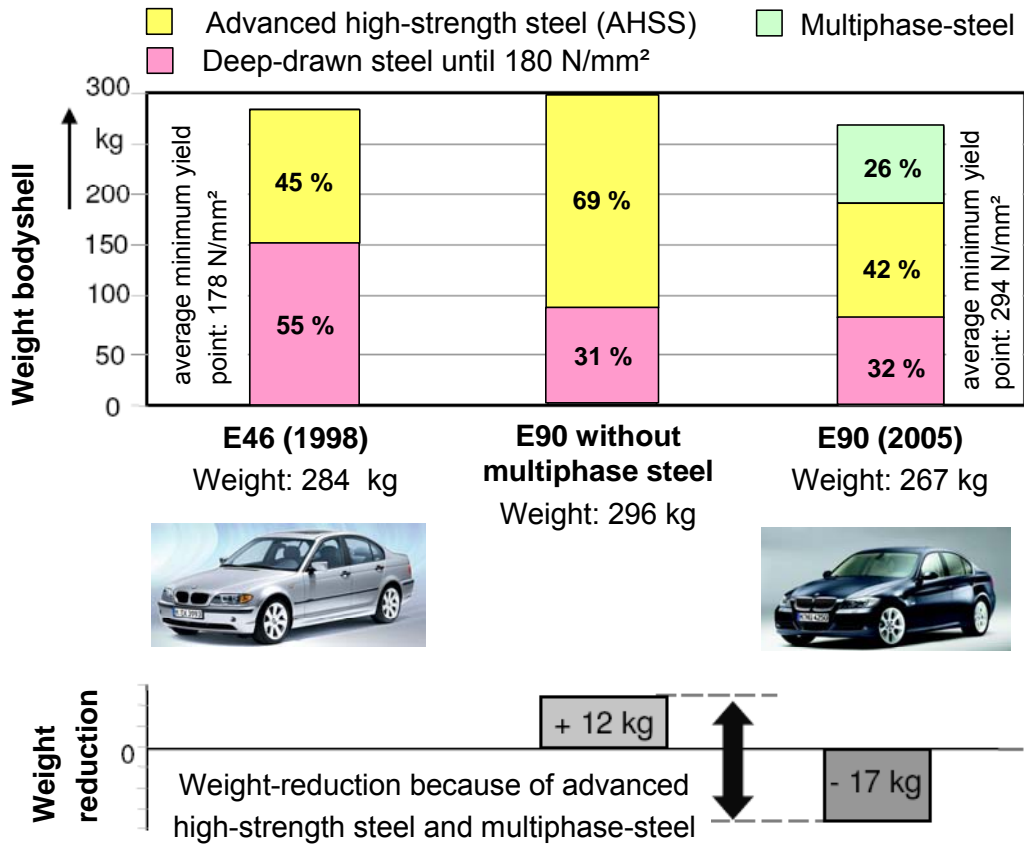
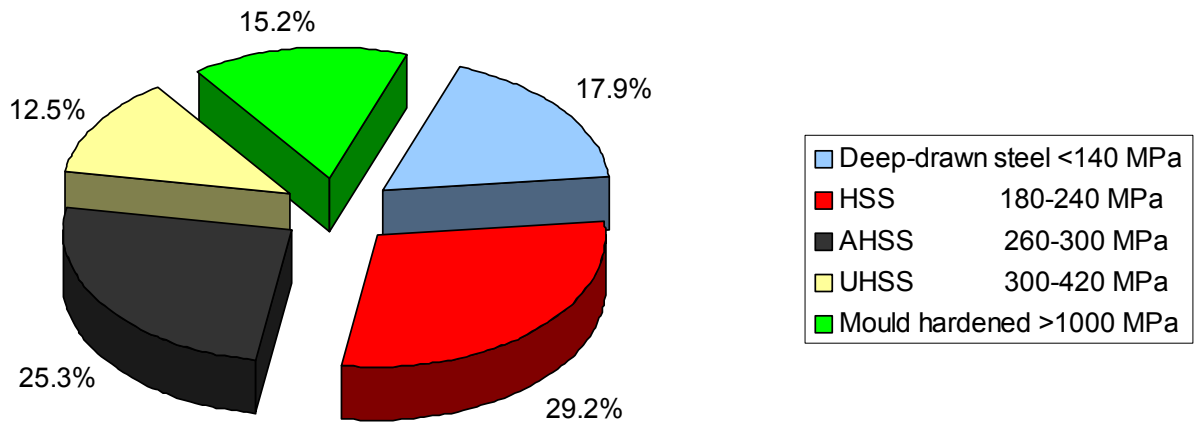Fig. 3-1:   Body of the BMW 3-Series [BRA05]

Fig. 3-2:   Material spreading of the Volkswagen Passat [STA05]

So the improvement of performance of recent vehicles especially regarding crash performance and higher stiffness lead to a slight increase of BIW-mass. This is shown at the example of the BMW 3-Series and the Volkswagen Passat (Fig. 3-3).
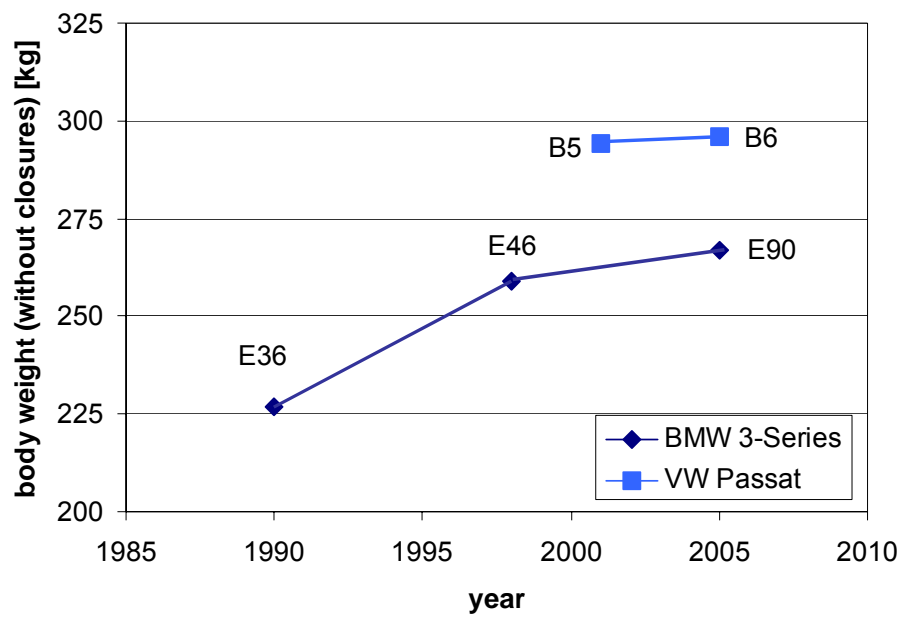
Fig. 3-3:   BIW weight development of BMW 3-Series and Volkswagen Passat

The crash performance of the VW Passat B5 (2001) reaches four stars in the EuroNCAP crash test and the Passat B6 (2005) reaches five stars.
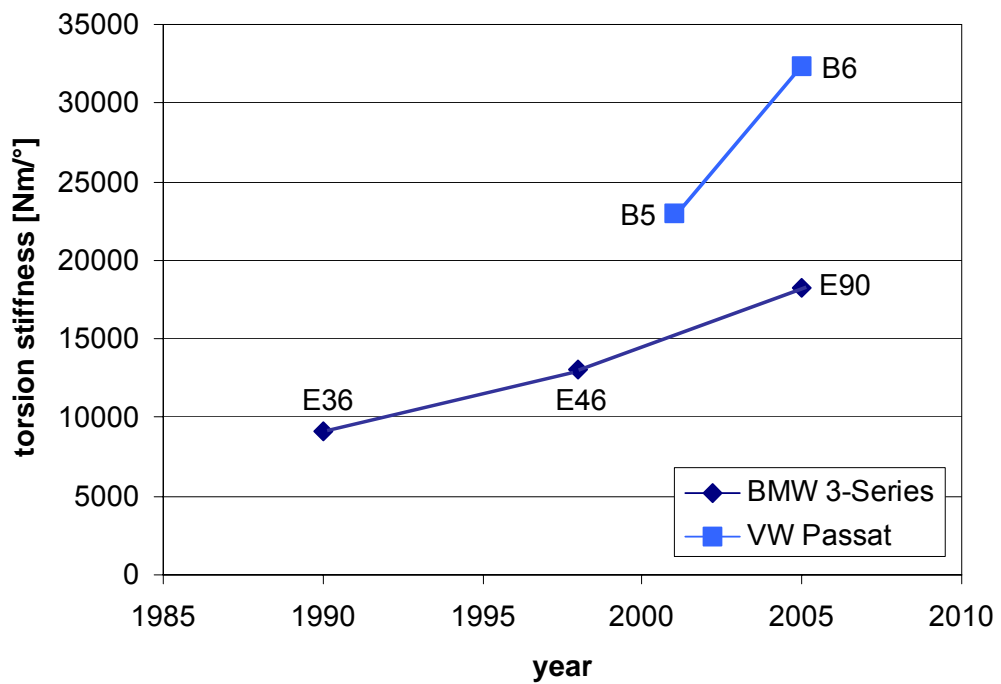

Fig. 3-4:   Torsion stiffness of BMW 3-Series and Volkswagen Passat

In the same way the is an improvement of crash performance at the BMW 3-Series. The E36 (1990) only reaches one star in the EuroNCAP test. The E46 (1998) already reaches four stars and the E90 (2005) reaches five stars. The same kind of performance improvement can be seen when regarding e.g. IIHS crash results.

Another indicator for performance is the torsion stiffness (Fig. 3-4). In the last years this parameter strongly improved at the BMW 3-Series as well as at the Volkswagen Passat. A comparison of Fig. 3-3 and Fig. 3-4 clarifies that in recent steel vehicles a slight increase of weight goes along with an enormous increase of stiffness.

So steel, especially advanced high-strength steels (AHSS) or higher steel grades, can improve the mass reduction potential of vehicle bodies. Another method to reduce the mass is to use a mixture of aluminium and steel. Some example vehicles can be found, e.g. the actual BMW 5-Series E60. Its aluminium front end is described in chapter 3.4 in detail.

3.1.1.2   Aluminium Body Structures

In recent years, new developments in body technology appeared to decrease the vehicles' body weight. One of these technologies is the aluminium space frame (ASF®). The first series vehicle with an aluminium space frame body was the Audi A8 (D2) in the year 1995.

Its body-in-white (BIW) weighs 198 kg without closures. In the year 2002 the actual Audi A8 (D3) entered the marked with a mass for the BIW without closures of 222 kg. This increase of mass was caused by a higher torsion stiffness and a better crash performance. The aluminium space frame consists of aluminium casting parts (e.g. B-pillar), sheet panels (e.g. tunnel) and extrusion profiles (e.g. door sill) (Fig. 3-5). Some of the extrusion parts (e.g. roof frame) are hydroformed. Punch riveting, MIG-welding and laser welding are used to join the body components in assembly [TIM03]. The Audi A8 reached production numbers of approx. 19000 vehicles in 2005.

Another vehicle with an aluminium space frame by Audi is the A2. It entered the market in 1999, and the production was stopped in 2005. In 2002, production figures of approx. 37 500 were reached. The BIW without closures weighs 145 kg. The aluminium space frame consists of sheet panels, extrusion profiles and vacuum die-cast parts (e.g. longitudinal beam front, A- and B-pillar) (Fig. 3-5). The extrusion profiles in the floor structure are calibrated by hydroforming. Joining techniques like punch riveting, MIG-welding, laser welding and roll folding in combination with bonding were used for assembly [ENG99].
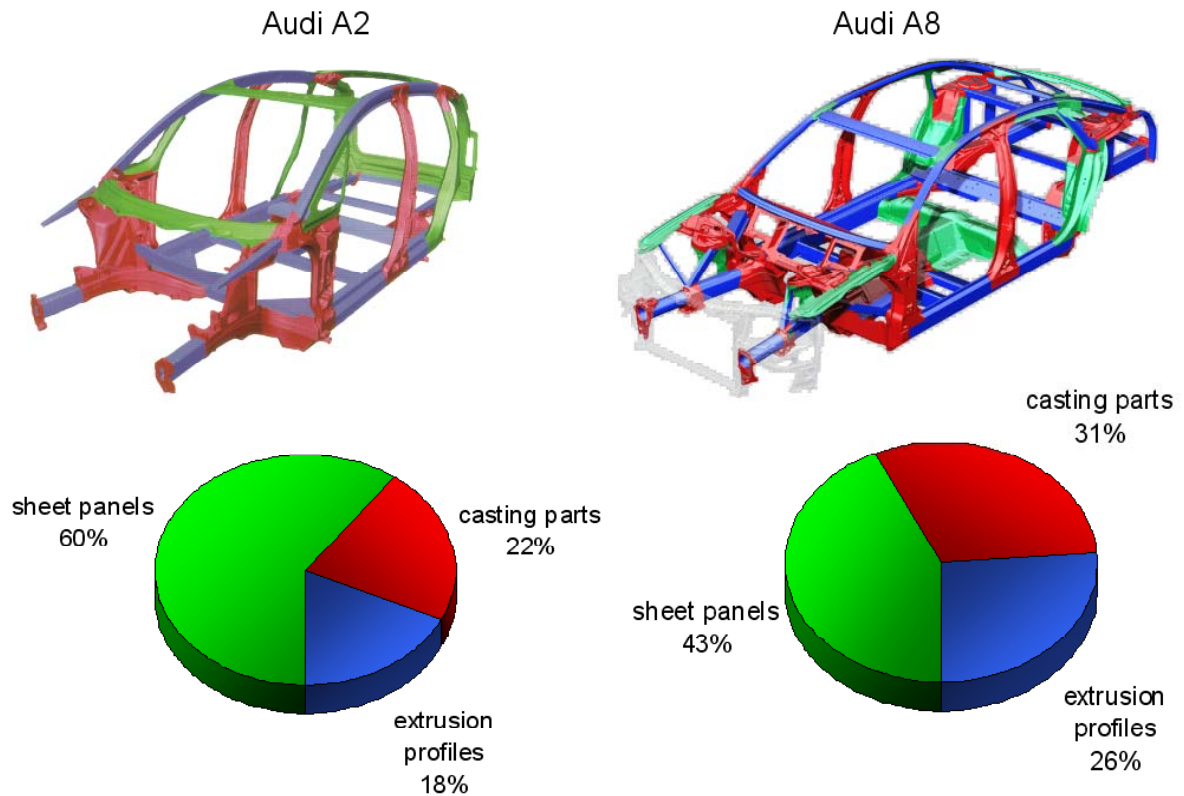
Audi A2

Audi A8

Fig. 3-5:   Aluminium space frame of Audi A2 and A8 [ENG99, TIM03]

Jaguar is another OEM who offers vehicles made of aluminium bodies. The Jaguar XJ and the new sports car Jaguar XK are both made of aluminium parts. The new Jaguar XK (Fig. 3-6) consists of a monocoque body construction made of aluminium casting parts and extrusion profiles with separate aluminium panels. As shown in Fig. 3-7 most of the aluminium body components (76 %) are manufactured by stamping [WHI06]. As a result the BIW weighs 287 kg (with closures). In comparison to the previous steel model a mass decrease of approx. 16 % was possible. For joining the structure punch riveting in combination with epoxy bonding are used [ICO06].

Fig. 3-6:   Jaguar XK

The Jaguar XK reaches production rates of about 8000 vehicles per year and the XJ about 13000 per year. The body of the actual XJ weighs 250 kg (without closures) what is a mass saving to the previous steel model of 40 %. At the same time stiffness was increased by 60 %. The XJ's aluminium monocoque body is assembled out of stamped parts, extrusion profiles and castings (Fig. 3-7). In this body the same joining techniques are used as in the XK [PAS03, SCH04].

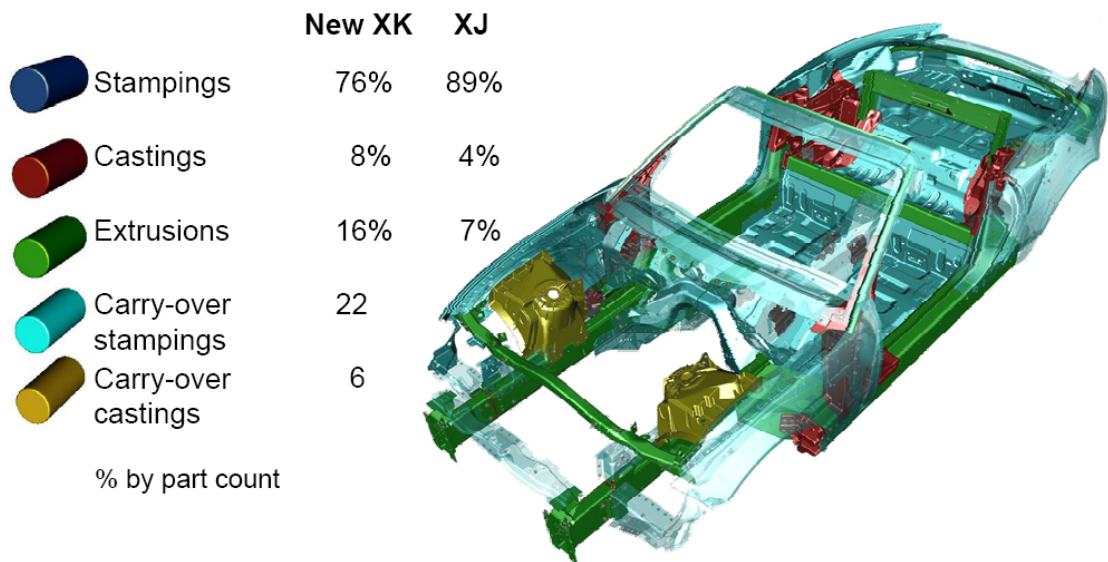|	New XK	XJ
Stampings	76%	89%
Castings	8%	4%
Extrusions	16%	7%
Carry-over stampings	22	
Carry-over castings	6	
% by part count		

Fig. 3-7:   Aluminium Application in the Jaguar XJ and the New Jaguar XK [WHI06]

Another example for a vehicle with an aluminium space frame is the Chevrolet Corvette C6 Z06. The Z06 is a special lightweight model of the Corvette C6. Approximately 33000 units of this vehicle are produced in 2006. To optimise lightweight design and retain chassis rigidity in the Z06 no removable roof for a fixed cast-magnesium structure is used. The engine cradle is also designed in magnesium.

Fig. 3-8:   Spaceframe Chevrolet Corvette Z06 [FRO06]

The frame beams are hydroformed parts with die-cast node points. The front fenders and wheelhouses are made of carbon-fibre reinforced plastics. In the underbody sandwich floorboards out of carbon-fibre and ultra-light balsa core are used. So the body weight of that car amounts 126 kg and a mass reduction of 62 kg was possible. This is a mass reduction of 30 % of the BIW weight in comparison to the previous steel model.

The development of BIW mass for the vehicles described above is shown in Fig. 3-9. In this chart the mass of the Jaguars is shown for a body-in white with closures and that of the Audi A8 and the Chevrolet Corvette is given for a body-in white without closures. The weight of the two Jaguars decreases because steel of the previous models (XK Mark I and XJ Mark II) was substituted by aluminium. Also regarding the Corvette Z06 there is a weight decrease between the C5 and the C6 because of the substitution of steel by aluminium, magnesium and plastics. At the same time performance increases.

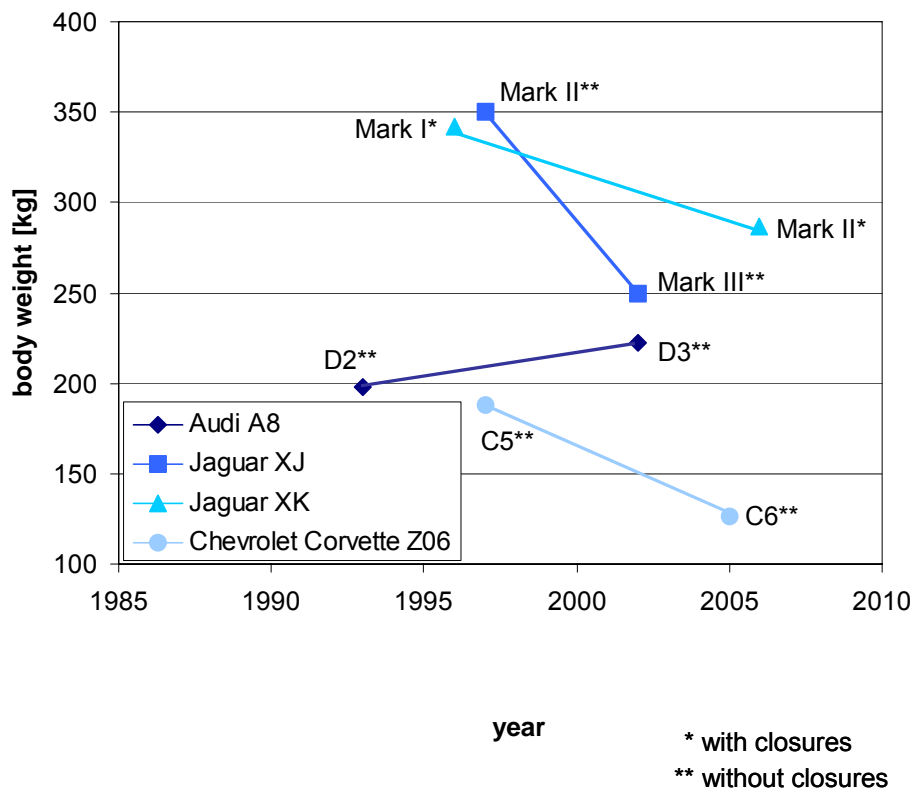Fig. 3-9:   BIW weight development of aluminium vehicles

As a result of the performance improvement of an aluminium body the Audi A8 D2 has a lower body weight than the D3. Both vehicles are designed in aluminium space frame design. So because of the improvement of crash performance and stiffness also the BIW mass increased. E.g. between the torsion stiffness of the D2 and D3 there is an improvement of 38 %.

Another point that has to be mentioned here is the manufacturing complexity of aluminium. Due to the long steel tradition aluminium designs are clean sheet of paper designs and designated as a light weighting program. A difference between aluminium and steel is, that aluminium needs custom built manufacturing facilities. So a change in design from steel to aluminium requires new investments.

3.1.2   Body Structures of Concept Vehicles

Possible future development trends concerning mass reduction of vehicle bodies can be clarified best with examples of actual concept cars.

3.1.2.1   ULSAB and ULSAB-AVC

The UltraLight Steel Auto Body (ULSAB) project was published in 1997. The target of this project was to reduce the body mass and improve stiffness at a high safety level. Therefore the concept body-in-white was developed in simulation and also in hardware. The ULSAB reference car was the 1994 Ford Taurus with a BIW weight of 271 kg. By high-strength, advanced high-strength and ultra-high strength steel as well as sandwich steel usage the weight was reduced to 203 kg (25 %). At the same time torsion stiffness increases by 80 % and bending stiffness by 52 % [ULT97].

The successor project of ULSAB is the UltraLight Steel Auto Body-Advanced Vehicle Concepts (ULSAB-AVC), published in 2004. In this project, a C-class and a PNGV-class vehicle (PNGV = Partnership for a New Generation of Vehicles) were optimised concerning several parameters like weight and stiffness (Fig. 3-10). The C-class refers to the European compact class with reference vehicles like the Opel Astra, VW Golf, Ford Focus etc. This class represents one third of the market volume in Europe. For this vehicle the Ford Focus is representative for vehicle dimensions and the Peugeot 206 for the vehicle weight target. The PNGV-class vehicle represents an US-American middle-class vehicle like the Chrysler Concorde, Ford Taurus, GM Lumina, etc. Contrary to these reference vehicles, which have a total weight of approx. 3200 lbs (1450 kg) each, the PNGV-vehicles should not weigh more than 2000 lbs (906 kg) [ULS04].

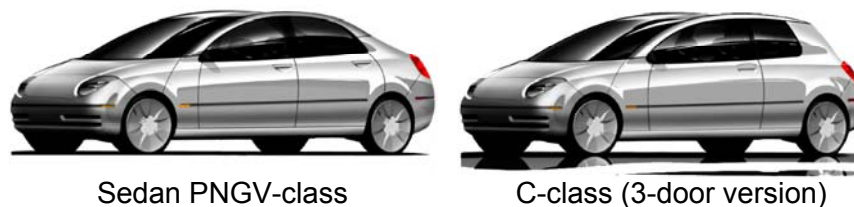Sedan PNGV-class   C-class (3-door version)

Fig. 3-10:   UltraLight Steel Auto Body – Advanced Vehicle Concept (ULSAB-AVC) [ULS04]

The main targets of the project were to fulfil safety standards, reach a cost-effective high volume suitability, reduce fuel consumption and improve environmental sustainability. These

targets were attained by application of modern high-strength multiphase-steels, innovative steel products, sophisticated production techniques and innovative construction principles [ULS04].

One of the targets in the project was to fulfil future crash requirements. Therefore ULSAB-AVC's body-in-white mass target was increased by 25 kg over the ULSAB body-in-white weight (243 kg) to take into account the estimated additional mass needed to meet the more severe crash events. Consequently the ULSAB-AVC C-class mass target was 268 kg, and the ULSAB-AVC PNGV-class mass target was 288 kg instead of 263 kg.

A detailed overview of the masses for both vehicles with gasoline engine as well as with diesel engine is given in Fig. 3-11, and the achieved values for structural performance are listed in Fig. 3-12 [ULS04].

	C-class		PNGV-class	
	Otto engine	Diesel engine	Otto engine	Diesel engine
Body in white [kg]	201.8		218.1	
Doors and closures [kg]	55.2		81.7	
Glazing [kg]	23.9		26.5	
Chassis [kg]	182.1		182.1	
Motor [kg]	122.1	150.9	123.7	152.5
Transmission [kg]	43.1	44.1	43.1	44.1
Interior [kg]	152.5		160.4	
Exterior [kg]	4.2		4.5	
Electronics [kg]	36.7		35.5	
Liquids [kg]	39.9	42.9	39.9	42.9
Miscellaneous [kg]	40.6	41.1	42.2	42.7
Coating [kg]	16.0		20.0	
Aerodynamic components [kg]	15.0		20.0	
Curb weight [kg]	**933.1**	**966.4**	**997.7**	**1,031.0**

Fig. 3-11:   Masses of ULSAB-AVC vehicles [ULS04]

As a result of the study, the platform concept with non-variable parts and parts made with the same tools could be realised including a concept for application of advanced high-strength steels (AHSS). By the application of innovative steel products, mass was decreased by 24.3 % in the ULSAB-AVC (PNGV-Class) and by 24.7 % in the ULSAB-AVC (C-Class) [ULS04].

	Target	C-class	PNGV-class
Global bending stiffness (N/mm)	11000	17050	17150
Global torsional stiffness (Nm/deg)	12000	14350	17400
First global bending eigenfrequency (Hz)	48	58	66
First global torsional eigenfrequency (Hz)	35	49	44
First local eigenfrequency front structure lateral (Hz)	> 55	> 70	> 70

Fig. 3-12:   Structural performance of ULSAB-AVC vehicles [ULS04]

The mass optimised body structure of the C-class vehicle weighs 201.8 kg, a 24.7 % mass reduction compared to the reference car. For the PNGV-class vehicle, that weighs 218.1 kg, a mass reduction of 24.3 % is achieved. The total PNGV-class vehicle weight is 966 kg compared to a characteristic weight for this class of 1150 kg. Analyses tend towards a five star rating for the EuroNCAP test [ULS04].

3.1.2.2   NewSteelBody

The NewSteelBody (NSB®) by ThyssenKrupp Steel (TKS) is also based on simulation and finally it was built partially as a demonstrator. The reference vehicle of the NSB® was the 1999 Opel Zafira with a body mass without closures of 317 kg. The main target of this project was to achieve equal structural performance at a lower mass level. The conceptual idea of the NSB® was to combine the advantages of innovative profile construction with elements of the classic unibody design. Therefore modern multiphase steel grades and new steel technologies are applied. As an alternative derivate to the van also a convertible is designed [OSB04].

At first a mass reduction of 10 % can be achieved by material substitution. A further mass reduction of up to 15 % is achieved by application of modern steel grades and tailored blanks without the requirement of new investments. The NSB® achieves a mass advantage with combination of innovative profile construction and conventional unibody construction of 24 % (= 75 kg) as primary weight saving. So, 43 kg mass reduction at the front axle and 32 kg reduction at the rear axle without shifting the axle load can be reached. The structure of the NSB® has a weight of 242 kg including 9.1 kg for miscellaneous parts not considered in the study. The NSB® has a total curb weight of 1318 kg. Furthermore there is no unfavourable shift of centre of gravity [OSB04].
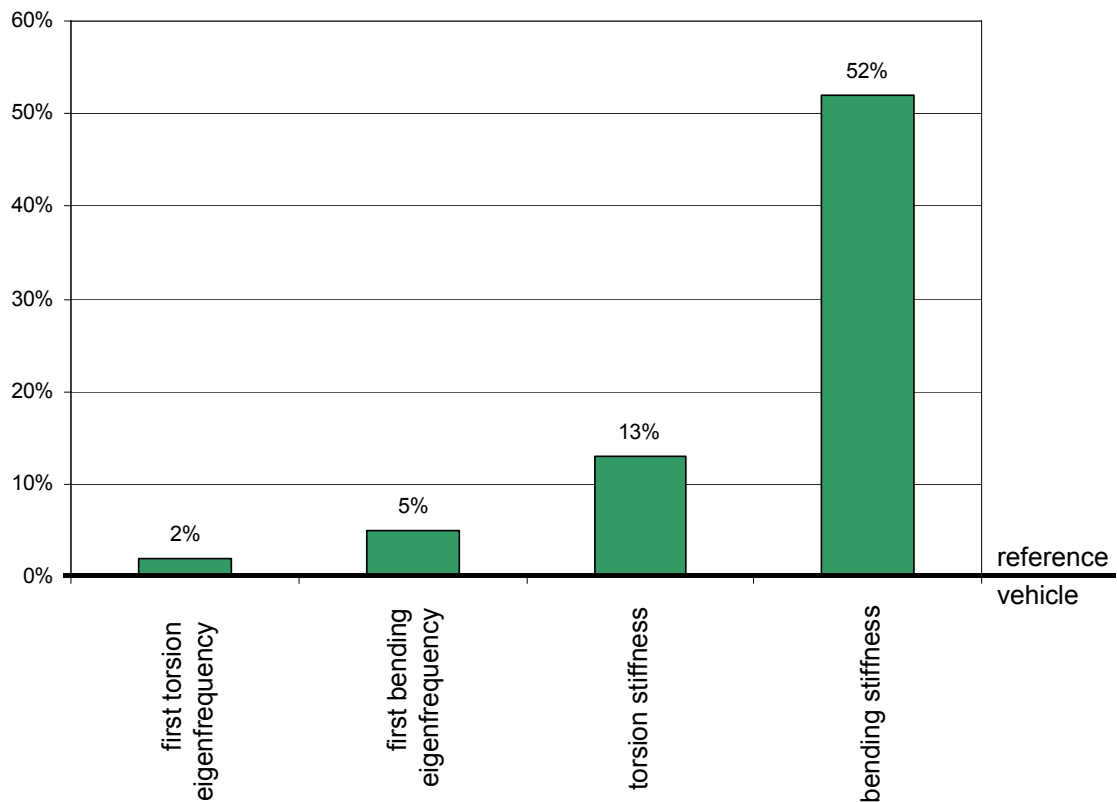
Fig. 3-13:   Structural performance of NSB$^®$ [OSB04]

Concerning body performance values like eigenfrequency and stiffness, the NSB$^®$ shows enhancements compared to the reference vehicle (Fig. 3-13). In addition the crash performance has been improved according to the reference vehicle. Using the profile intensive construction simplifies the creation of derivates. The cost analysis was based on a volume of 200000 units per year over 6 years [OSB04].

3.1.2.3   Arcelor Body Concept

In 2004 the steel company Arcelor published its Arcelor Body Concept (ABC) (Fig. 3-14) which is a model for a C- or D-class vehicle using new kinds of steel. As perimeter 63 % of the whole BIW with closures have been considered for this study. This perimeter contains the underbody, the upper body and the front doors [CAZ04]. This study was based on simulation and finally a demonstrator was built.

The virtual reference car for the ABC has to fulfil high crash standards (e.g. EuroNCAP with 5 stars). It has a mass of the BIW with front doors of 313 kg. So, the 63 % perimeter of this vehicle has a mass of 197 kg [CAZ04].

Fig. 3-14:   Arcelor Body Concept (ABC) [CAZ04]

By usage of sandwich steels, advanced high-strength steels and tailored blanks, a mass of 155 kg could be reached for the 63 % perimeter of the ABC without significant changes of the reference vehicle architecture. This means a mass reduction of 21 % in the perimeter. The remaining 37 % of the BIW have not been studied. In the ABC perimeter the most mass could be reduced in the underbody (26 %), followed by the upper body (19 %). In the front doors, 18 % mass could be saved. At the same time global stiffness increases by 9 % and the stiffness to weight ratio is improved by 20.7 %. All this leads to a cost increase of 8 % [CAZ04].

3.1.2.4   Ford AIV

Using Alcan's aluminium vehicle technology Ford North America has developed a fleet of 40 aluminium intensive vehicles (AIVs) in 1997. Based on the mid-sized Taurus/Mercury the use of aluminium has resulted in a bodyshell that is 47 % (182 kg) lighter than its steel equivalent. With the use of aluminium throughout the powertrain components the total weight saving in curb weight is 318 kg over the steel Taurus. So the AIV is 21.1 % lighter in curb weight than the Taurus. Information about costs have not been found.

Fig. 3-15:   Ford AIV

The essential difference between the Ford AIV and other aluminium cars is the processes used in construction. Whilst most other aluminium vehicles utilise low volume technologies Ford test vehicles were produced using conventional high volume processes in conjunction with Alcan's AVT structural bonding system. The use of bonding in conjunction with

conventional spot welding technology maximises the weight saving and also improves structural performance with increased bending and torsional stiffness, and increased fatigue resistance [LEA02]. Furthermore the AIV essentially matched and improved on the crash performance of the regular steel production vehicle so, that the results for the Audi A8 are very similar to those for the Ford AIV [WHE02].

3.1.2.5   Ford P2000

In the P2000 program by Ford, scientists and engineers are developing lightweight, family-sized vehicles and adding various powertrains including an aluminium intensive direct-injection engine, hybrid electric, and fuel cell electric drives.

The first P2000 design concept for the direct hydrogen vehicle is a theoretic study of 1997. It is an aluminium concept car with two derivates, a station wagon and a sedan. A demonstrator was not built. In this vehicle, aluminium sheet closure panels, a cast aluminium front by Alcoa and rear shock towers are used as well as aluminium tailor-welded blanks. For joining the body Alcan's Aluminium Vehicle Technology is used to join aluminium by welding [AEG97].

Fig. 3-16:   Ford P2000 [SZE99]

Thereby a structure weight of 136 kg, a mass of the body-in-white with windows and interior of 398 kg and a curb weight of 907 kg has been targeted for this concept. The reference car, a Ford Taurus of the year 1997, has a body weight of 387 kg with closures and a curb weight of 1505 kg. So a theoretic reduction of the body weight by 40 % in curb weight has been targeted in this concept study [AEG97, FRE01]. Information about performance (e.g. crash, stiffness etc.) and costs of this vehicle are not published. So no exact statements of the mass potential of this concept are available.

After this concept the P2000 sedan and the P2000 SUV is developed in this program. The P2000 SUV is the beginning of the technical innovations aimed at developing a virtually

emissions-free fuel cell vehicle. It has an aluminium body-in-white, suspension and closures. These provide major weight savings of as much as 50 % compared with former designs. The P2000 SUV retains the same torsion and bending stiffness as conventional vehicles [FOR99a].

The P2000 sedan (Fig. 3-17) is the other vehicle that is realised in this program. It has an aluminium body-in-white, suspension and closures and also carbon fibre, magnesium and titanium are used for some body parts. As a result the P2000 sedan is 40 % lighter than the Taurus sedan [FOR99b], but the curb weight is 0.6 % higher than that of the Taurus because of the higher mass for the hybrid drivetrain.

Fig. 3-17:   Ford P2000 sedan [FOR05]

3.1.2.6   Lotus APX

The Lotus APX (Aluminium Performance Crossover) is the first complete vehicle built on the new Versatile Vehicle Architecture (VVA). Versatile Vehicle Architecture is Lotus Engineering's attempt to take platform sharing to allow automakers to make unique vehicles with high commonality and lower investment. The APX (Fig. 3-18) is at the same time the first crossover sport utility vehicle (SUV) by Lotus. All significant components and structural items are made from Aluminium.

Fig. 3-18:   Lotus APX [LOT06]

Its underbody is rivet-bonded aluminium, consisting of high-pressure die-castings, stampings and extrusions. It uses advanced assembly techniques, including adhesive bonding, self-piercing rivets and flow-drill screws for construction. The self-piercing rivets are used in a similar way to spot welding on a former steel shell, with the flow-drill screws used for single-sided access on closed sections. Both suffice to hold the structure together during the adhesive cure cycle, and contribute to the performance of the structure during both static and dynamic impact conditions. The heat-cured high strength structural adhesive is the main joining medium and used in combination with the mechanical fasteners, produces an immensely strong, durable joint and a lightweight shell with exceptional torsional stiffness [LOT06].

This results in a curb weight of 1570 kg of the APX. It fulfils actual requirements on NCAP targets for crash, pedestrian impact, torsion, bending and modal stiffness targets. Comparable to this vehicle in steel design is the Volvo XC70, that has a curb weight of 1764 kg. So the Lotus APX is 11.0 % lighter in curb weight than the Volvo. Unfortunately the BIW mass of the APX is not available as well as further performance issues and costs.

3.1.3   Conclusions

A comparison of mass reduction potential can be clarified best by a comparison of different cars within a separation of vehicle classes.

Fig. 3-19 gives an overview of weight reduction potential in the luxury class. The three vehicles compared here have nearly equal height, length, width and they are notchback limousines.

	Picture	Body Design	Year	Weight BIW [kg]
Jaguar XJ Mark II		former steel design	1997	350 (without closures)
BMW 7-Series		recent steel design with aluminium parts (side covering, hood, fenders)	2001	+ 0.9 % 353 (without closures) 430 (with closures)
Jaguar XJ Mark III		recent aluminium design with attached aluminium parts	2002	- 28.6 % 250 (without closures)
Audi A8 (D3)		recent aluminium design: aluminium-space-frame with attached aluminium parts	2002	- 37.1 % - 37.1 % 222 (without closures)

Fig. 3-19:   Overview of weight reduction - luxury class

Basis for the comparison of steel vehicles with aluminium vehicles in this class are the Jaguar XJ Mark II, that is designed in former steel design, and the BMW 7-Series, that is designed in recent steel design. The BIW of the Jaguar XJ Mark III is 28.6 % lighter than the previous model and the Audi A8 (D3) 37.1 % lighter than that the XJ Mark II. Because only a slight mass increase can be found between the XJ Mark II and the BMW 7-Series, the mass decrease between the BMW 7-series and the Audi A8 (D3) is also 37.1 %. The influence of optimised steel design can not be shown here, because all example vehicles belong to smaller vehicle classes. Data for crash performance of these vehicles are not published by EuroNCAP.

In the upper middle class the comparison of vehicles using recent steel design, partially mixed with aluminium structures (e.g. the aluminium front end of the BMW 5-series), and the ULSAB-AVC, that represents optimised steel design is possible. Fig. 3-20 shows that by optimised steel design a mass reduction of 29.9 % would be possible. By consequent usage of optimised steel parts in the non-body parts a reduction of curb weight by 36.6 % would be possible.

	Picture	Body Design	Year	Weight BIW [kg]
Mercedes Benz E-Class		recent steel design with aluminium parts (hood, fenders, boot lid, front and rear modul)	2003	328 (without closures)
BMW 5-Series		recent steel design with aluminium front structure and aluminium parts	2004	281 (without closures)
Audi A6		recent steel design with aluminium parts (hood, luggage compartment partition, fenders ...)	2004	319 (without closures)
Peugeot 607		recent steel design	1999	316 (without closures)
Reference Car Subcompact		recent steel design	-	311 (without closures)
				- 29.9 %
ULSAB-AVC PNGV-Class		optimised steel design	2004	218 (without closures)

Fig. 3-20:   Overview of weight reduction – upper middle class

This indicates the high mass reduction potential of optimised steel design. Concerning crash performance the BMW 5-Series reaches four stars in the EuroNCAP crash test and the Audi A6, the Citroen C6 and the Mercedes E-Class reach five stars. The ULSAB-AVC fulfils

actual crash requirements by adding 25 kg to the body mass. So this virtual vehicle would also reach four or five stars in EuroNCAP [ULS04].

On the basis of the Ford Taurus 1997 several concept vehicles are developed (Fig. 3-21). One is the ULSAB-AVC of the PNGV-Class that reaches a weight reduction of 24 % in the body-in-white without closures. For the same reference vehicle two further concept vehicles with an aluminium body exist. The Ford P2000 Sedan is 40 % lighter than the reference vehicle and the Ford AIV is 47 % lighter.

	Picture	Body Design	Year	Weight BIW [kg]
Ford Taurus		former steel design	1997	387 (with closures)
				- 47.0 %
Ford AIV		former aluminium design	1998	205 (with closures)
				- 40.0 %
Ford P2000 Sedan		former aluminium design	1999	232 (with closures)

Fig. 3-21:   Overview of weight reduction – upper middle class

Further examples for a comparison of aluminium vehicles and recent steel vehicles can be found in the sports car class. Unfortunately a direct comparison of the Chevrolet Corvette with the steel reference car of this class is not possible, because no data for the BIW with closures is available (Fig. 3-22). Concerning the previous Corvette Z06 C5 this means a weight reduction of body weight of 30.0 % and a weight reduction of curb weight of 2.0 %.

	Picture	Body Design	Year	Weight BIW [kg]
Chevrolet Corvette Z06 C5		former steel design with FRC hardtop	1998	188 (without closures)
				- 30.0 %
Chevrolet Corvette Z06 C6		recent aluminium body with aluminim and magnesium parts, FRC hardtop	2006	126 (without closures)

Fig. 3-22:   Overview of weight reduction – sport cars

Another comparison in of the BIW mass of sport cars is shown in Fig. 3-23. The reference vehicle for steel cars is given by the Mercedes SL and the BMW 6-Series. The aluminium

BIW of the Jaguar XK weighs 21.4 % less than that of a reference car, that partially contains aluminium parts (e.g. the BMW 6-Series). A comparison of crash performance is not possible, because data are not published by EuroNCAP.

	Picture	Body Design	Year	Weight BIW [kg]
MB SL		**recent steel design**	**2001**	**360 (with closures)**
BMW 6-Series		**recent steel design with aluminium front structure and aluminium parts**	**2004**	**370 (with closures)**
Reference Car Sportcars		**recent steel design**	**-**	**365 (with closures)**
				- 21.4 %
Jaguar XK		**recent aluminium design with attached aluminium parts**	**2006**	**287 (with closures)**

Fig. 3-23: Overview of weight reduction – sportcars

Fig. 3-24 shows the potential of the ULSAB-AVC in the compact class. A reference car with a former steel body has a body weight of 286 kg and a reference car with recent steel design has a body weight of 272 kg. So the recent steel design reference car is 4.9 % lighter than the former steel design reference car. The optimised steel body of the ULSAB-AVC has a 25.7 % lower BIW weight than a recent steel design BIW and a 37.1 % lower curb weight than a former steel design BIW. Concerning crash performance the two former steel design vehicles (Ford Focus and Fiat Stilo) get four stars in the EuroNCAP crash test. The recent steel design vehicles (BMW 1-Series and Volkswagen Golf 5) achieve fife stars. Also the ULSAB-AVC could reach four or five stars [ULS04]. The torsion stiffness of the reference cars and the ULSAB-AVC are in the same range (approx. 14000 Nm/°).

Furthermore an example of an optimised steel design car is given by the NSB®. It is based on a compact class van. An example for a former steel design compact class van is the Opel Zafira A with a BIW mass of 300 kg. The Ford Focus C-Max is designed in recent steel design and has a BIW mass of 298 kg (Fig. 3-25). So it is 0.7 % lighter than the Zafira. In comparison to the Focus C-Max the NSB® has 25.7 % less in BIW weight and in comparison to the Zafira it has 37.1 % less BIW mass.

	Picture	Body Design	Year	Weight BIW [kg]		
Ford Focus		former steel design	1998	274 (without closures)		
Fiat Stilo		former steel design	2001	297 (without closures)		
Reference Car Compact		former steel design	-	286		
				- 4.9 %		
VW Golf V		recent steel design	2003	284 (without closures)		
BMW 1-Series		recent steel design	2004	260 (without closures)		
Reference Car Compact		recent steel design	-	272		
				- 25.7 %		- 37.1 %
ULSAB-AVC C-Class		optimised steel design	2004	202		

Fig. 3-24:   Overview of weight reduction – compact class

	Picture	Body Design	Year	Weight BIW [kg]		
Opel Zafira		former steel design	1999	300 (without closures)		
				- 0.7 %		
Ford Focus C-Max		recent steel design	2002	298 (without closures)		
				-18.8 %		- 19.3 %
NSB		optimised steel design	2003	242 (without closures)		

Fig. 3-25:   Overview of weight reduction – compact class vans

An overview of weight reduction of the sub-compact class is given in Fig. 3-26. It shows that the body structure of the Audi A2 is 34.2 % lighter than that of an average recent steel

6rh0098.doc

reference car in this class. The Ford Fiesta, the Opel Corsa and the Audi A2 reach four stars in the EuroNCAP crash test. So crash performance is equal.

	Picture	Body Design	Year	Weight BIW [kg]
Ford Fiesta		**recent steel design**	**2002**	**239 (without closures)**
Opel Corsa		**recent steel design**	**2003**	**240 (without closures)**
Reference Car Subcompact		**recent steel design**	**-**	**240 (without closures)**
Audi A2		**former aluminium design (aluminium-space-frame) with attached aluminium parts**	**1999**	**158 (without closures)**

- 34.2 %

Fig. 3-26:   Overview of weight reduction - sub-compact class

The production cars mentioned above are very limited examples of the mass saving potential of combining AHSS and efficient design. The potential of mass reduction by substitution of former and recent steel design through optimised steel design at concept projects is shown in Fig. 3-27 and Fig. 3-28.

25.0 %   24.7 %   24.3 %   24.3 %   21.0 %*

* 63% perimeter of complete body
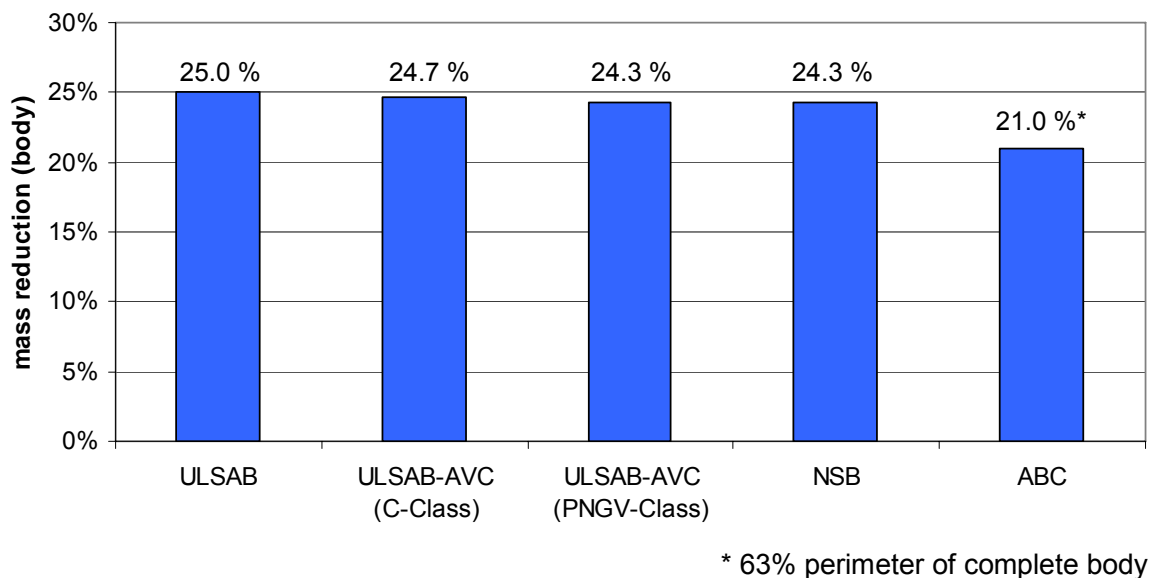
Fig. 3-27:   Mass reduction for BIW without closures with optimised steel design

The range of possible mass reduction realised by concept cars like the ABC, ULSAB, ULSAB-AVC and NSB are between 21 and 25 % compared to the reference vehicles designed in a former steel body. This approves the statement given in Fig. 3-27 that recent steel bodies can achieve a 25 % lighter body weight compared to a former steel body. Detailed information of these concept cars are summarised in Fig. 3-28. An overview of the aluminium concept vehicles is not given, because no detailed information is available.

Concept	Year	Class	Reference Vehicle	Weight Structure Reference Vehicle [kg]	Weight Structure [kg]	Weight Saving Structure
ULSAB	1997	upper middle	Ford Taurus '94	271	203	68 kg = - 25.0 %
ULSAB-AVC	2004	compact	C-class vehicle	268	202	60 kg = - 24.7 %
ULSAB-AVC	2004	PNGV	PNGV-class vehicle	288	218	60 kg = - 24.3 %
NSB	2003	compact	Opel Zafira '99	317	240	77 kg = - 24.3 %
ABC	2004	compact & middle	C- / D-class vehicle	197*	155*	42 kg = - 21.0 %*

* 63% perimeter of complete body

Fig. 3-28:   Mass reduction for BIW without closures with optimised steel design in detail

Design	Vehicles
former steel design	Ford Taurus '94, Ford Taurus '97, BMW 3-Series E36, Renault Megane '96, VW Passat B5, Opel Zafira A, Chevrolet Corvette Z06 C5, Jaguar XJ Mark II, Peugeot 607, Ford Focus, Fiat Stilo, Opel Corsa, Ford Fiesta
recent steel design	Audi A6, MB E-Class, MB SL, BMW 1-Series, BMW 3-Series E90, BMW 5-Series E60, BMW 6-Series, BMW 7-Series, Renault Megane 2003, VW Passat B6, Ford Focus C-Max, VW Golf V
optimised steel design	ULSAB, ULSAB-AVC, NSB®, ABC
former aluminium design	Audi A8 (D2), Audi A2, Ford AIV, Ford P2000 Sedan
recent aluminium design	Audi A8 (D3), Corvette Z06 C6, Jaguar XJ Mark III, Jaguar XK Mark II

Fig. 3-29:   Analysed vehicles

This chapter shows that lightweight design of body structures is possible with aluminium as well as with steel. All results of this chapter are gathered together in Fig. 3-30. The mass for the BIW given in Fig. 3-19 to Fig. 3-26 are compared regarding the special design. An overview of the analysed vehicles is given in Fig. 3-29.

The reference design for this weight comparison is the former steel. The other vehicle body designs that are analysed in this study are referred to this reference design concerning the mass reduction potential. To compare the different design type with each other, it is necessary to introduce a BIW-mass index, which is visualised in Fig. 3-30. This mass index achieves a value of 100 for the former steel design.

Based on the analysed data, the BIW-mass index of a recent steel vehicle has to be estimated in the next step. Within a comparison of former steel design vehicles with recent steel design vehicles a weight increase of 18 % can be indicated. This is based on the body mass development of the BMW 3-Series E36 to the E90 (see Fig. 3-3). The reason for that can be found in an increase of size, stiffness and crash requirements. In vehicles like the Volkswagen Passat there is a mass increase of only 0.6 % (see Fig. 3-3). Due to these reasons the range of the weight increase of recent steel design is estimated between 0 % and 18 % in comparison to former design. So, this results in a range of the BIW-mass index between 100 and 118.

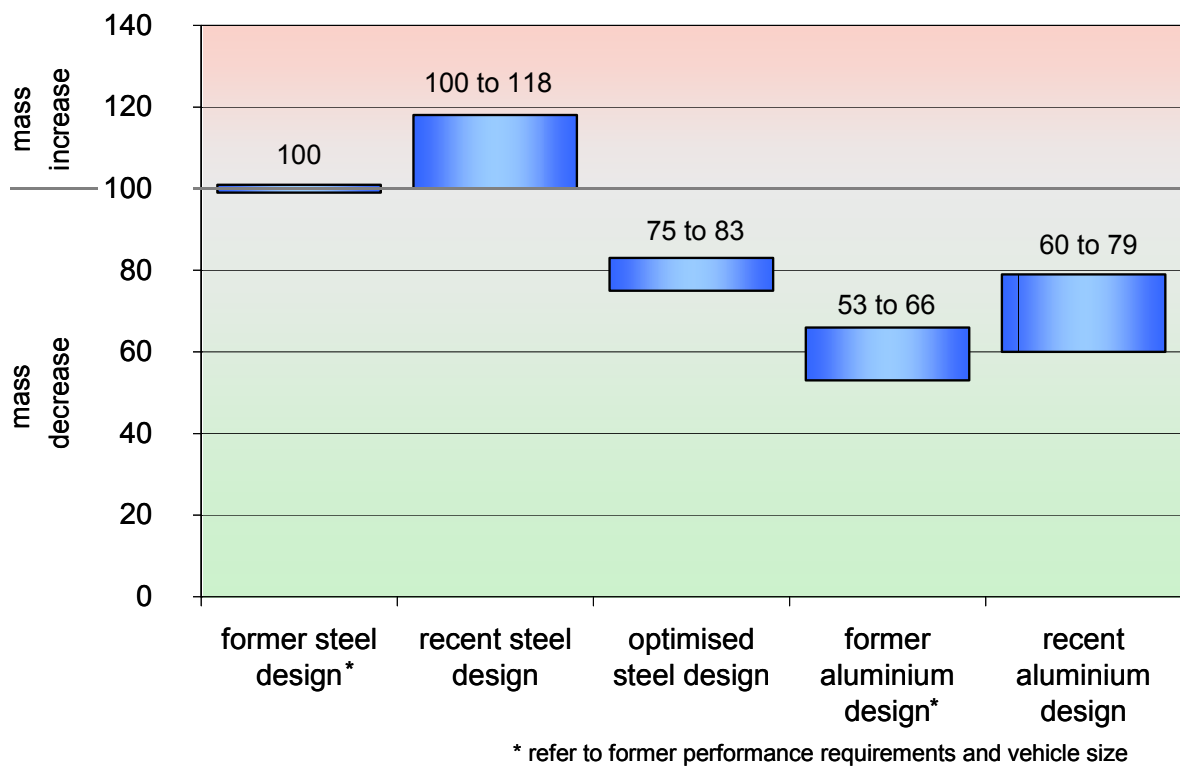Fig. 3-30:   Range of BIW-mass index for analysed vehicles

6rh0098.doc

Fig. 3-30 also shows that optimised steel design (e.g. ULSAB) offers the potential to decrease the vehicle body mass up to 25 % in comparison to the former steel design (see Fig. 3-27). This results in a mass index of 75. In the ULSAB-AVC study the reference vehicle is a Ford Taurus '97 with improved stiffness and crash performance. The virtual improvement of a former steel design vehicle like the Ford Taurus '97 was realised in the ULSAB-AVC study by the addition of 25 kg mass to fulfil higher crash performance. So, these improved vehicles belong to the recent steel design vehicles. Because of that the ULSAB-AVC must be compared with recent steel design vehicles like those shown in Fig. 3-24. The ULSAB-AVC C-Class is about 28 % lighter than a compact class reference car in a recent steel design. An analogous estimation is possible in the upper middle class, where the ULSAB-AVC PNGV-Class is about 30 % lighter (Fig. 3-20). If this percentage is referred to the mass index of 118 of a recent steel body, the mass index of an optimised steel body is 83. So the mass index of an optimised steel design can be found in a range between 75 and 83. This means, by optimised steel design a mass reduction of 17 % to 25 % is possible in comparison to former steel design.

In former aluminium design vehicles (e.g. the Ford AIV) the body mass of their reference cars is reduced of up to 47 % (see Fig. 3-21). A more conservative approach is the comparison of the Audi A2 with recent reference cars in the subcompact class (see Fig. 3-26). This comparison indicates a mass reduction of 34 %. So the range of mass reduction by former aluminium design lies between 34 % and 47 % in comparison to the former steel design. This results in a range for the BIW-mass index between 53 and 66 (Fig. 3-30).

At the example of the Audi A8 D2 and the D3 a mass increase of 12 % can be found. It is caused by an increase in performance and size. So, the D2 is a representative of former aluminium design and the D3 of recent aluminium design. This results in a first estimation for the BIW-mass index between 60 and 74 for the recent aluminium design. Another vehicle in this design class is the Jaguar XJ Mark III. It has a 40 % lower body mass than the XJ Mark II in former steel design (Fig. 3-9). This confirms the lower limit of BIW-mass index for recent aluminium design of 60. The comparison of recent sport cars in Fig. 3-23 with a Jaguar XK Mark II shows that about 21 % mass decrease by an aluminium body is possible. Thus, the mass reduction potential of recent aluminium designs can be estimated between 21 % and 40 % in comparison to former steel designs. That means the BIW-mass index of recent aluminium design can be found in a range of 60 to 79 (Fig. 3-30).

Fig. 3-30 allows a comparison of recent steel design with recent aluminium design as well as the comparison of optimised steel design with recent aluminium design. First, the recent steel design is compared with the recent aluminium design. Out of the BIW-mass index chart follows an average value for recent steel design of 109. For the recent aluminium design this results in an average value of 70. This results in a mass reduction potential between this two design steps of 36 %.

Finally the range of mass reduction between optimised steel design and recent aluminium design is analysed (no optimised aluminium design is available). The BIW-mass index value

for recent aluminium design stays on 70. The average value for BIW-mass index of optimised steel design is 79. This results in an average weight advantage for aluminium of about 11 %.

3.2   Hoods

In this chapter the contents of two hood studies of the Forschungsgesellschaft Kraftfahr-wesen mbH Aachen (fka) are described to point out mass differences of steel and aluminium hoods. Additionally the influences of new pedestrian protection requirements on hoods are shown.

3.2.1   Simulation of Hoods

At fka a study about the influence on mass of steel and aluminium was conducted [WOH05]. A digitised steel hood of a VW Golf V is examined in this study and several load cases are considered in a FE-simulation. The most important load cases for hoods are lateral stiffness, transversal stiffness and torsion stiffness. These load cases are shown in Fig. 3-31. In addition the buckling behaviour is analysed in this study. The main target was to determine the weight of the hoods by simulation at an equal performance.
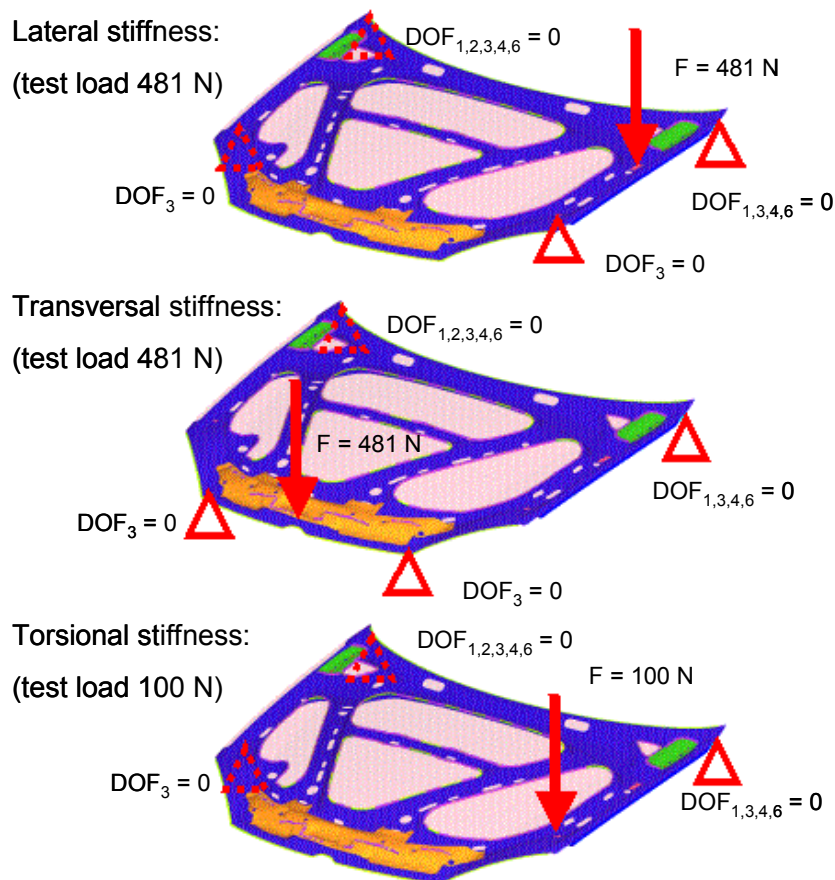
Fig. 3-31:   Load cases for structural stiffness

Within the study the reference steel hood is virtually substituted by an aluminium hood design with adapted sheet thicknesses. Thereby the topology and topography remains. The reference steel hood has an outer panel thickness of 0.72 mm and an inner panel thickness of 0.65 mm. In the resulting aluminium hood higher sheet thicknesses (outer panel 1.20 mm; inner panel 1.25 mm) are necessary in order to provide at least the same performance.

The outer panel is rather responsible for dent requirements and the inner panel assures the structural stiffness. In order to test the dent resistance and the oil canning of the hoods, two different specimens are used. For the oil canning test a cylindrical steel plate with a diameter of 50 mm and for the dent resistance test a hemispherical steel indenter with a diameter of 25 mm are used in simulation. Again the same performance as of the reference steel hood is achieved.

The reference steel hood has a weight of 12.61 kg and the average estimated material costs amount to 8.89 €. As a result the aluminium hood weighs 8.10 kg and the average estimated material costs amount to 16.63 €. So, a mass reduction of 36 % is connected with a material cost increase of 87 %.

3.2.2   Benchmark of Hoods

In a benchmarking study of fka 20 aluminium and seven steel hoods (all original parts from series production vehicles) were benchmarked concerning torsional, lateral and transversal stiffness as well as for the weight and the size of the hoods.

Within this chapter two different approaches are described, which deal with relationship of mass and structural performance. In the first approach the performance is related to mass and size. In this point aluminium and steel hoods are compared by structural performance and mass performance (mass per hood size).

In the second approach mass is related to structural performance and size. Thereby the performance of steel hoods is decreased to the level of aluminium hoods and then they are compared by mass and size.

The basis for these two approaches are several real tests, which are executed to determine the structural performance of the hoods. In this study lateral stiffness, transversal stiffness and torsional stiffness are tested. The result data is normalised for comparison. This normalisation is necessary to compare the different hood sizes.

In the first approach the calculation of normalised stiffness is related to mass performance for the results of the real test. The mass performance points up the relationship between the mass and the surface of the hood. This value should reach preferably low values. As a result aluminium hoods exhibit higher structural performance at comparable mass and size of 25 % in average.

The basis for the second approach are the results of structural tests and the corresponding normalised stiffness values of the steel and aluminium hoods. The average structural performance of the normalised stiffness of the aluminium hoods is about 27 % lower than that of the steel hoods.

In the next step of this second approach the performance of the steel hoods is adapted to that of the aluminium hoods by decreasing the sheet thickness virtually (Fig. 3-32). This is done with the help of a FE-simulation based on the data of the ULSAC steel hood.
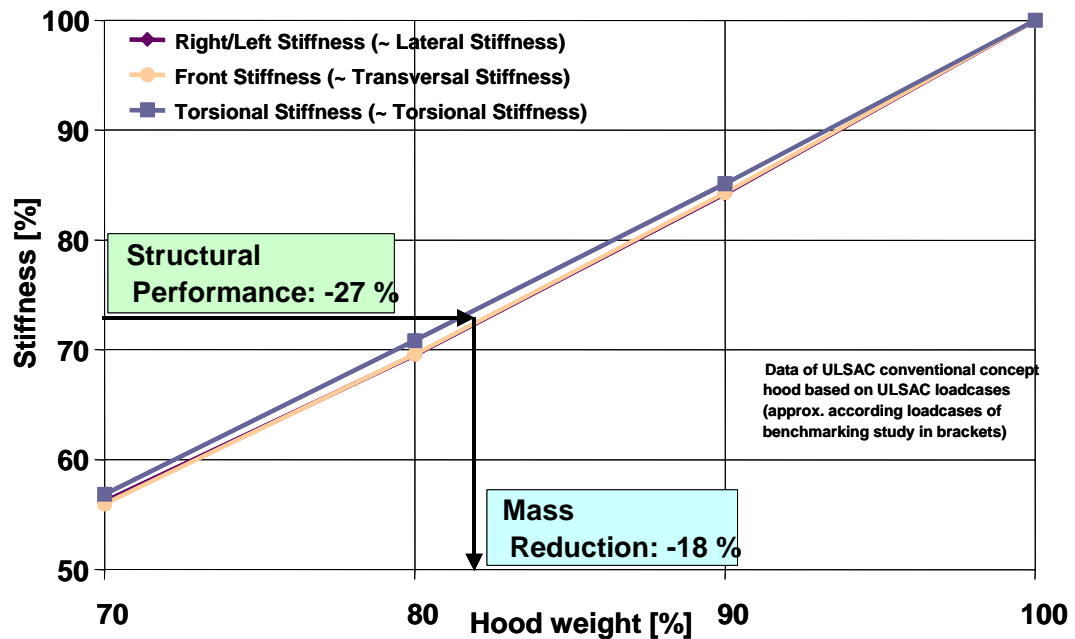
Fig. 3-32:   FE-simulation chart

The value for the average structural performance of the stiffness can be used as input for the FE-simulation chart. In Fig. 3-32 the curves for lateral, transversal and torsional stiffness are itemised. By this chart it is possible to calculate the allowed mass reduction of a steel hood to reach the lower stiffness level of an aluminium hood. Based on the measured 27 % lower structural performance a mass reduction of 18 % is determined by the help of the FE-simulation result chart. So, if the steel hood is 18 % lighter than the original steel hood, it reaches the same stiffness level as the aluminium hood.

The weight of the steel hood after the 18 %-weight reduction is used for the further calculation. This calculation considers the hood sizes (mass performance). For that calculation the average surface for the steel and the aluminium hoods is used. Regarding only the mass, the examined aluminium hoods are in average 32 % lighter than the steel hoods and the corresponding mass performance of the aluminium hoods is 41 % lower (Fig. 3-33).

Mass (Basis)	Average of **Steel** hoods	-32 % →	Average of **Aluminium** hoods
Mass Perf. (Basis)		-41 % →	
Mass (18 % reduction)		-17 % →	
Mass Perf. (based on 18 % red.)		**-28 %** →	
avg. surfaces of steel hoods: 1.35 m² / avg. surfaces of aluminum hoods: 1.56 m²			

Fig. 3-33:   Results of second approach of benchmarking study

When reducing the mass of the steel hoods by the determined 18 % the same performance level for both materials is reached. If these hoods are compared the mass reduction amounts to 17 % and the corresponding mass performance of aluminium is 28 % lower than that of steel.

3.2.3   ULSAC Hoods

In the UltraLight Steel Auto Closures Study (ULSAC) especially body parts like hoods, doors and trunk-lids were studied by FE-simulation concerning the mass reduction potential at equal performance values. Basis for the project was a benchmark of several 1997 vehicles (e.g. Audi A6, BMW 528I, Ford Probe, Porsche Boxster, VW Golf, VW Passat etc.). Like in the hood benchmark the parameter mass performance is used again.

The conventional hood consists of the outer and inner panel. In this study two kinds of hoods are analysed, a conventional hood and a hood with integrated front grill. Out of the analysis of several hoods that are already on market results an average mass performance of 11.5 kg/m². By optimisation results the ULSAC hoods which are shown in Fig. 3-34.

	Benchmark (kg/m²)		Target (kg/m²)	ULSAC	
	Range	Average		(kg/m²)	(kg)
Hood - Conventional*	8.8-14.2	11.5	8.0	7.9	13.3
Hood - Grill Integrated*				7.9	13.7
Hood - Conventional**				8.5	14.3
Hood - Grill Integrated**				8.4	14.7

* with steel sandwich material inner panel

** with sheet steel inner panel

Fig. 3-34:   Mass comparison [IIS00]

For both configurations (conventional and grill integrated) a ULSAC hood with inner panel out of sandwich material and one with an inner panel out of sheet steel is developed. The ULSAC hoods with sandwich material are 31 % lighter than a conventional hood and the sheet steel hoods are 26 % to 27 % lighter.

To determine torsional rigidity, the hood is constrained at the hinges and at one of the front bump stops while loaded vertically. For bending stiffness, the hood is constrained at the hinges while the load was applied at the front edge. To determine side beam stiffness, the hood was constrained at the hinges and bump stops while vertical loads were applied independently at each side beam at the centreline of the section. As a result, the targets for torsion rigidity and bending stiffness are exceeded for both hood configurations as shown in Fig. 3-35.

Structural performance (conventional)

Load case	Target (N/mm)	Actual (N/mm)
Torsional rigidity	≥ 5.8	6.3
Bending stiffness	≥ 4.5	7.2

Structural performance (grille integrated)

Load case	Target (N/mm)	Actual (N/mm)
Torsional rigidity	≥ 5.8	6.6
Bending stiffness	≥ 4.5	7.4

Fig. 3-35:   Structural performance [IIS00]

3.2.4   Conclusion

The performed hood studies point out, that the substitution of steel by aluminium allows a mass reduction of approx. 25 to 36 %. This mass reduction goes along with a material cost increase of up to 87 % (based on averaged material prices of November 2005).

3.3   Bumper

Bumpers are mainly loaded for bending when hitting an obstacle. In chapter 2.2.4 the load case 3-point bending is described as machanic formula. This load case describes the loading of a bumper at best. Although there is less data for bumper weight available, the following comparison is chosen for demonstration. But the available data serves well for illustration, because the selected parts are from the same vehicle type of the same OEM.

In recent years, some OEMs were using aluminium, whereas in previous years, steel was usually applied. Currently, some OEMs, e.g. BMW, have switched back to steel solutions. Fig. 3-36 shows one example for the comparison of an aluminium and a steel rear bumper, both BMW parts. The aluminium bumper is used in the old BMW 5-Series (E39) that has a curb weight of 1570 kg. It is made out of one aluminium part and has a mass of 4 kg. The steel bumper is used in the actual BMW 5-Series (E60) that has a curb weight of 1545 kg. It is made out of one steel part and has a mass of 3.7 kg. So, the new steel bumper is 8 % lighter than the aluminium design.

Fig. 3-36:   Comparison of aluminium and steel rear bumper

A detailed overview of material and weight allocation in the front and in the rear bumper of the BMW E39 and the E60 shows Fig. 3-37. Including the crash boxes, the potential for weight reduction by usage of a steel bumper can be shown. In the rear bumper a weight reduction of 22.1 % is realised by steel.

Body part		E39		E60	
		weight [kg]	material	weight [kg]	material
Rear end	Bumper	4.0	aluminium	3.7	steel
	Crashelement (left/right)	1.81 + 1.92	steel	1.16 + 1.16	steel
	Sum	7.73		6.02	-22.1 %

Fig. 3-37:   Bumper of BMW E39 and E60 [ETK06]

This is one example that a steel bumper might get lighter than an aluminium bumper. Especially UHSS have the potential for realisation of light weight bumpers made out of steel. On the other hand in most cases aluminium bumpers are lighter than comparable steel bumpers, yet [WEL05]. But this weight advantage of an aluminium bumper might decrease in future, as the example of BMW shows.

3.4   Front Structure

Especially the front end is very important for crash performance of a vehicle. The influence of steel and aluminium structures in this vehicle area are described in this chapter.

3.4.1   Benchmarking of a Front Structure

A comprehensive automotive benchmarking study of aluminium and steel front structures was conducted by fka. The body structures of the recent BMW 5-Series (E60) and the previous model (E39) were analysed. The front structures were disassembled and all parts were analysed regarding weight, dimensions, thicknesses and joining techniques.

To analyse the front structure it is systematically divided into five areas (Fig. 3-38). The fire wall area (FW), the wheelhouse area, divided in left and right side (WHL, WHR) and the longitudinal beam area, also divided in left and right side (LBL, LBR).

Fig. 3-38:   Allocation of front structures

The analysis of the BMW E60 shows that special technologies like castings, extrusions and hydroformed parts are used in addition to aluminium sheet metal. The detailed results of this benchmark are listed in Fig. 3-39. The analysed BMW E60 front structure has an 11 kg weight advantage compared to the E39. In the analysed E60 front structure, 63 % of the weight consists of aluminium parts and 37 % of steel parts. In the E39 all parts of the front structure are made of steel. The number of parts in the analysed E60 front structure is about 18 % higher compared to the BMW E39. Six sheets are applied in the BMW E60 to adapt the aluminium component of the body to the steel part.

	Weight [g]					Parts [#]				
	WHL	WHR	FW	LBL	LBR	WHL	WHR	FW	LBL	LBR
BMW E39	10829	10877	16978	10812	10787	22	21	31	15	13
BMW E60	10587	10636	11658	8175	8175	31	32	39	9	9
Variation	-2%	-2%	-31%	-24%	-24%	+41%	+52%	+26%	-40%	-31%

	Weight [g]					Parts [#]				
	Front Struct.	Steel		Aluminium		Front Struct.	Steel		Aluminium	
BMW E39	60282	60245	100%	-	-	102	100*	98%	-	-
BMW E60	49231	18134	37%	30955	63%	120	43*	36%	72*	60%
Variation	-18%					+18%				

* Differences due to existing plastic parts

Fig. 3-39:   Comparison of both structures

In addition the performance of the complete body structure is tested. The BMW E60 body structure torsion stiffness, i.e. front structure, passenger compartment and rear structure, is about 47 % higher than at the E39. When considering only the body structure and windows, the difference is 15 %. The additional parts, like subframe, strut tower bar, bumper and IP-support, have a high influence on the torsion stiffness of the BMW E60. In contrast, they do not contribute much to the E39's performance. The bending stiffness of the BMW E60 body structure, including all additional parts is 41 % higher than at the E39. Concerning the crash performance both 5-Series models achieved four stars in the EuroNCAP test rating.

A cost analysis of both BMW front structures was conducted. An extensive cost model was generated, based on the technical input of a very detailed analysis of the front structures. The cost model assumes series production of the vehicles and allows variations of input parameters. The calculation of the results is done with a standardised production volume of 225000 units per year. The cost analysis showes that the E60 front structure is about 59 % more expensive concerning material, forming and assembly costs.

The results show that the high stiffness values of the E60 are caused by the much stiffer steel passenger compartment and the more influencing additional parts. No special advantage with regard to body structure stiffness can be attributed to the usage of aluminium. Consequently, the same performance is also possible using steel in the front structure.

3.4.2   Lightweight Front End Structures

The lightweight front end structure study by the Auto/Steel Partnership demonstrates in simulation and hardware the mass reduction potential of rail/bumper system by substitution of conventional steel through AHSS [ASP06]. The reference car for the project is a recent 5-passenger mid-size sedan. The solution for the new rail/bumper system is constrained by the package of the reference vehicle.

The existing vehicle's performance in crash as well as in static and dynamic stiffness should maintain on the same level. It has to fulfil the requirements of the frontal NCAP 35 mph rigid barrier impact and of the IIHS 40 mph deformable barrier offset impact as well as static and dynamic stiffness requirements.

The baseline design of the bumper rail assembly contains the bumper and the two rails. The last ones consist of several rail elements and reinforcements. Together with the bumper it has a mass of 39.23 kg.

In the new design (Fig. 3-40) all parts are made of dual phase steel (DP800 or DP980). The bumper rail assembly is designed as a laser welded blank (LWB), so it is one part with different areas of thickness. Most reinforcements are eliminated. This assembly weighs 30.46 kg, so it is 22.4 % lighter than the conventional one. At the same time it is providing the same performance concerning crash and stiffness.
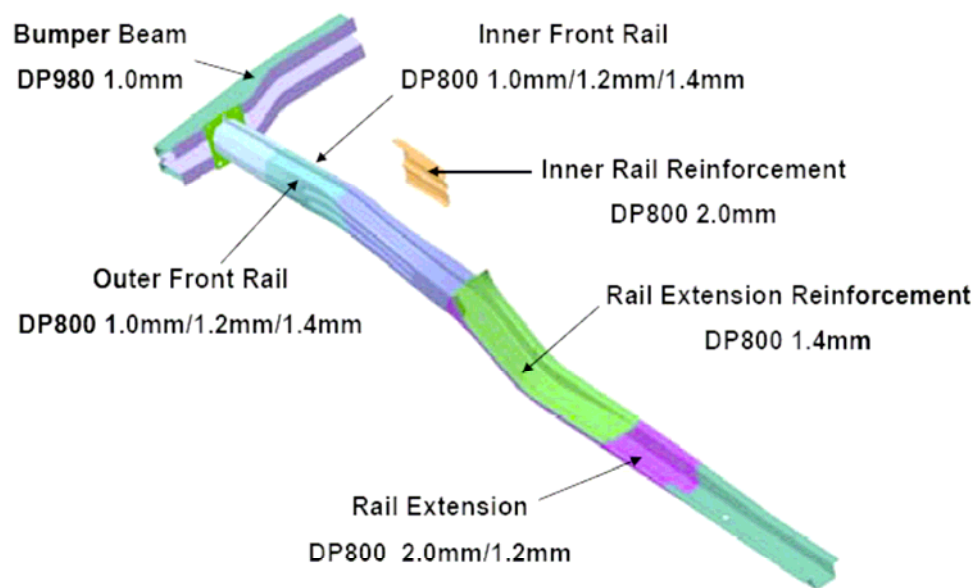
Fig. 3-40: New design – Bumper/Rail Assembly [ASP06]

The AHSS rail and bumper design was validated by conducting an real NCAP 35 mph rigid barrier impact test. The bumper and the front section of the rails crushed completely and there was no significant deformation of the A-Pillar, B-Pillar, roof rails and rail extension rear. The B-pillar acceleration peak of the new AHSS design was lower than that of the baseline design. Overall, the new AHSS design had an NCAP performance similar to that of the baseline design.

Fig. 3-41: NCAP 35 mph crash test [ASP06]

4   Summary and Outlook

In this study the mass reduction potential of steel and aluminium was analysed. In order to give a general impression about the mass reduction potential several applications and concepts were compared. For a basic comprehension the mechanic fundamentals were explained and referred to vehicle demands.

The most important load cases on a vehicle body are bending stiffness, torsion stiffness and tensile strength as well as three-point bending. Analytical formulas explaining this basic load cases were investigated in detail.

Fundamental analysis of selected simple load cases (e.g. bending stiffness and three-point bending) and mild steel only (lowest strength steel) shows the potential for aluminium to achieve 50 % or even 60 % mass reduction (if no package space restrictions are applied). Under these conditions the often-stated assumption that mass can be reduced by up to 50 % by the application of aluminium could be supported – but not for a complete vehicle structure – only for the two selected simple load case bending stiffness and torsion of an open profile. Concerning package requirements all analysed aluminium grades need 40 % more package space than the analysed steel grades in that two load cases.

On the other hand, fundamental analysis of other selected simple load cases and the use of high strength steel shows that aluminium has a mass reduction potential equivalent or less than steel. E.g. in the two load cases tensile strength and three-point bending steel grades like MS 1250/1520 and aluminium 7021 T6 both can reach a mass reduction of 80 % in comparison to mild steel. Thus, the relevance of package demands at same performance increases. E.g. for closed profiles there is no mass difference at equal performance between aluminium and steel, but steel needs three times less wall thickness (package) than aluminium. In these load cases steel is as light as aluminium.

In actual vehicle body structures, where load cases are much more complex than selected simple cases, neither of the above fundamental scenarios are achievable for itself. But the load cases are fundamental parameters for crash simulation and topology optimisation of a body structure, because the definition of a suitable compromise between stiffness, crash and further body requirements is the main challenge in the development of a body structure. So, there are no available direct comparisons of vehicle structures, however this study evaluates current production and concept vehicles in both steel and aluminium design and makes mass comparisons.

The results indicate that aluminium may achieve 11 % to 36 % mass reduction depending on whether it is compared to optimised steel design or to recent (non optimised) steel design. This results out of the fact that concept steel cars like the UltraLight Steel Auto Body, the NewSteelBody® or the Arcelor Body Concept show that within a consequent usage of new steel grades and optimised steel design a mass reduction of up to 25 % in comparison to former steel design. A comparison of this optimised steel design with recent aluminium design leads to the conclusion that a mass reduction of 11 % by aluminium is possible. In the

aluminium design of recent vehicles steel applications of the predecessor are substituted by aluminium. A mass reduction of 21 % to 36 % to the former steel design is possible, here.

Since new vehicle design are globally moving toward more optimised design and greater usage of high strength and advanced high strength steel (typical new BIW-structures use 50 % to 60 % percent high and advanced high strength steels), it must be concluded that the mass reduction potential for aluminium compared to steel will be closer to the lower end (11 %) of the range.

The performed hood studies pointed out, that the substitution of steel by aluminium allows a mass reduction of approx. 25 % to 36 %. This mass reduction goes along with a material cost increase. The UltraLight Steel Auto Closures study showed, that also in steel design mass reduction is possible by a consequent usage of advanced high-strength steels.

Today, for bumper material steel is as usual as aluminium. Aluminium is mostly used to decrease the mass. But on the other hand it is also possible to design steel bumpers that a up to 8 % lighter than a corresponding aluminium bumper.

The analysis of front structures shows that a lower weight for this area of approx. 18 % is possible with aluminium. This goes along with a higher amount of parts (+18 %) and higher costs for material, forming and assembly (+59 %). On the other hand it is also possible to decrease weight by an optimised steel design. A weight reduction of about 22.4 % for a bumper rail system is possible. At the same time the number of parts was decreased.

So new developments on the steel side should help to reduce further the gap in the weight saving potential, that is established at some applications. Examples could be found were steel nearly reaches an equal weight performance like aluminium. But also the development of aluminium technology processes. Aluminium tailor welded blanks are in development [VAN05], that should help to optimise weight of aluminium bodies as well as new aluminium grades that are specially designed for their application. Also on the steel side new materials like TWIP-steel might help to use steel more weight efficient.

5   Formula Symbols and Indices

A_{CS} cross section area [mm]

A_P package area of a profile [mm²]

$A_{P,al}$ package area of an aluminium profile [mm²]

$A_{P,st}$ package area of a steel profile [mm²]

b   width [mm]

b_m width at neutral axis [mm]

D   outer diameter of the hollow profile [mm]

d   inner diameter of the hollow profile [mm]

d_m mean diameter of the hollow profile [mm]

E   modulus of elasticity [N/mm^2]

E_1 modulus of elasticity (material 1) [N/mm^2]

E_2 modulus of elasticity (material 2) [N/mm^2]

F   load [N]

F_B bending force [N]

F_{max} maximum load [N]

F_{PL} plastic load [N]

F_T torsion force [N]

f   deflection [mm]

G   modulus of shearing [N/mm^2]

G_1 modulus of shearing (material 1) [N/mm^2]

G_2 modulus of shearing (material 2) [N/mm^2]

h   height of a beam [mm]

h_1 height of a beam (material 1) [mm]

h_2 height of a beam (material 2) [mm]

h_{al}	height of an aluminium profile [mm]
h_m	height at neutral axis [mm]
h_{ref}	height of a beam (reference material) [mm]
h_{st}	height of a steel profile [mm]
I	geometrical moment of inertia [m^4]
I_a	axial moment of inertia [mm^4]
$I_{a,1}$	axial moment of inertia (material 1) [mm^4]
$I_{a,2}$	axial moment of inertia (material 2) [mm^4]
I_p	polar moment of inertia [mm^4]
$I_{p,c}$	polar moment of inertia of a thin-walled closed round profile [mm^4]
$I_{p,o}$	polar moment of inertia of a thin-walled open round profile [mm^4]
I_t	torsional moment of inertia [mm^4]
$I_{t,1}$	torsional moment of inertia (material 1) [mm^4]
$I_{t,2}$	torsional moment of inertia (material 2) [mm^4]
l	length [mm]
M_T	torsion moment [Nm]
m	mass [kg]
m_1	mass material 1 [kg]
m_2	mass material 2 [kg]
m_{al}	mass aluminium profile [kg]
m_{ref}	mass reference material [kg
m_{st}	mass steel profile [kg]]
R	outer radius [mm]
R_e	yield strength [N/mm^2]
R_m	resistance to extension [N/mm^2]

R_{m1}	resistance to extension (material 1) [N/mm^2]
R_{m2}	resistance to extension (material 2) [N/mm^2]
r	(inner) radius [mm]
r_m	central radius [mm]
t	thickness [mm]
t_1	thickness (material 1) [mm]
t_2	thickness (material 2) [mm]
t_{al}	thickness of an aluminium profile [mm]
t_{ref}	thickness (reference material) [mm]
t_{st}	thickness of a steel profile [mm]
W_0	axial resistance moment [mm^3]
α	profile coefficient
φ	angle [deg]
η_3	correction factor
σ	stress [N/mm^2]
ρ	density [kg/m^3]
ρ_1	density (material 1) [kg/m^3]
ρ_2	density (material 2) [kg/m^3]
υ	Poisson number [1]

6   Literature

[AEG97]   N.N.
             Highlights of Aluminium in Auto Design
             Automotive Engineering, December, 1997

[AHL05]   AHLERS, M. / ELVERT, J.
             Der neue 3er BMW
             BMW AG, München
             EuroCarBody 2005, Bad Nauheim, 2005

[ASP06]   N.N.
             Lightweight Front End Structure
             Phase I & II – Final Report
             Homepage: www.a-sp-org
             Auto/Steel Partnership, Michigan, 2006

[AUT02]   N.N.
             Der neue Opel Vectra
             Automobilindustrie, No. 2, 2002

[BRA05]   BRAUNSPERGER, M.
             Die Karosserie des neuen BMW 3ers – Innovation Stahlleichtbau
             BMW AG, München
             Tag der Karosserie, Aachen, 2005

[CAZ04]   CAZES, C. / GATARD, G. / LUCIANI, M.
             Steel solutions for a better world
             Arcelor body concept: ABC project
             Arcelor Auto
             EuroCarBody 2004, Bad Nauheim, 2004

[CHE06a]   N.N.
             Chevrolet Corvette Z06
             http://www.autosieger.de
             Autosieger.de, München, 2006

[CHE06b]   N.N.
             Chevrolet Corvette Z06
             Homepage: http://www.chevrolet.com
             General Motors Corporation, Detroit, 2006

[COR06]   N.N.
             Hompage: www.corusgroup-duffel.com
             Corus, Duffel, 2006

[DIE92]   DIEKER, S. / REIMERDES, H.-G.
             Elementare Festigkeitslehre im Leichtbau
             Donat Verlag, Bremen, 1992

[ETK06]   N.N.
             ETK – Elektronischer Teilekatalog BMW
             BMW, München, 2006

[FOR99a]   N.N.
             Ford P2000 SUV shows breakthrough technologies on a lightweight sport
             utility
             Ford Motor Company, Detroit, 1999

[FOR99b]   N.N.
             Ford P200 – A practical vision for the future
             Ford Motor Company, Detroit, 1999

[FOR05]   N.N.
             Homepage: www.media.ford.com
             Ford Motor Company, Detroit, 2005

[FUG05]   FUGANTI, A. / TORELLI, A. / AIMO, G.
             The new Fiat Punto
             Fiat Auto SpA, Italy
             EuroCarBody 2005, Bad Nauheim, 2005

[FUR03]   FURRER, P.
             Cost-efficient lightweight car body design with aluminium
             Alcan Automotive, Alcan Technology & Management Ltd.
             Euromotor Body, Aachen, 2003

[FUR05]   FURRER, P.
             New aluminium sheet materials for lightweight car body design
             Novelis Technology AG
             Euromotor Body, Aachen, 2005

[FRE01]   FRETTY, P.
             Car wars
             Advanced Manufacturing, Volume 3, 2001

[FRO06]   FÖRDERREUTER, A.
             Ferrari F430 Spaceframe
             Alcoa Automotive, Soest
             The Consistent Lightweight Automobile 2006, Bad Nauheim, 2006

[GAS02]   GASPER, M. / SCHNEIDER, D. / STREHL, R.
Die Karosserie des neuen Opel Vectra C
Adam Opel AG, Rüsselsheim
EuroCarBody 2002, Bad Nauheim, 2002

[ENG99]   ENGELHART, D. / MÖDL, C.
Die Entwicklung des Audi A2, ein neues Fahrzeugkonzept
in der Kompaktwagenklasse
Audi AG, Ingolstadt, 1999

[ICO06]   N.N.
IISI Branding and communication strategy
Competitive analysis: Aluminium use in Jaguar XK
ICON Creative Technologies Group - Communications Committee
International Iron and Steel Institute, Ann Arbor (MI, USA), 2006

[IIS00]   N.N.
UltraLight Steel Auto Closures – Project Overview
International Iron and Steel Institute, 1998

[IIS06a]   N.N.
ULSAB Results Summary
Hompage: http://www.ulsab.org/ulsab/11.htm
World Auto Steel - International Iron and Steel Institute, Middletown, 2006

[IIS06b]   N.N.
Advanced High Strength Steel Application Guidelines
http://www.worldautosteel.org/pdf_ahssg/1aAHSSDef.pdf
World Auto Steel - International Iron and Steel Institute, Middletown, 2006

[LEA02]   LEANEY, P. / MARSHALL, R.
The manufacturing challenge for automotive designers
Loughborough University, 2002

[LOT06]   N.N.
Lotus APX
Homepage: www.carbodydesign.com, 2006

[NIC05]   NICOLAS, B.
Eine bahnbrechende Innovation für den Leichtbau von Fahrzeugen
Arcelor Auto, 2005

[OSB04]   OSBURG, B. / PATBERG, L. / GRÜNEKLEE, A. / FLÖTH, T. /
             GROSSE-GEHLING, M. / MEBUS, H. / PATON, A.
             NSB® - NewSteelBody, Technische Dokumentation
             ThyssenKrupp Steel, Duisburg, 2004

[PAL06]   PALM, F.
             New High Strength AlMgSc Type Profile Materials for Future Metallic Aircraft
             Structures
             EADS Deutschland GmbH, Munich, 2006

[PAS03]   PASCHEK, L.
             Die Aluminiumkarosserie des neuen Jaguar-Topmodells XJ
             ATZ, 2003

[SCH04]   SCHLOTT, S.
             Aus dem Flugzeugbau: Ultrafeste Leichtbautechnik
             Rohkarosserie um 40 Prozent leichter
             Automotive Materials, No. 1, 2004

[STA05]   STÄRKER, K. / STRUBE, C. / CORDES, R. / HILLMANN, J.
             The new PASSAT
             The Challenge of Combining Steel Lightweight Design and Passive Safety
             Volkswagen AG, Wolfsburg
             Aachen Colloquium, 2005

[SZE99]   SZEWCZYK, M.
             Ford Motor Company, 1999

[TIM03]   TIMM, H. / KOGLIN, K.
             Der neue Audi A8 – innovativer Leichtbau in Perfektion
             Audi AG, Ingolstadt
             EuroCarBody 2003, Bad Nauheim, 2003

[ULS04]   N.N.
             ULSAB-AVC
             Advanced Vehicle Concepts
             Project Presentation
             International Iron and Steel Institute, Middletown, 2004

[UFF06]   UFFELMANN, D.
             Hochfeste Aluminiumbleche, Eigenschaften und Verarbeitung
             Austria Metall Aktiengesellschaft, Braunau-Ranshofen
             The Consistent Lightweight Automobile 2006, Bad Nauheim, 2006

[WAL05]   WALLENTOWITZ, H.
Structural Design of Vehicles
Institut für Kraftfahrwesen Aachen, Aachen, 2005

[WEL05]   WELO, T. / HOLTHE, R.
Bumper System Designs based on Formed Aluminium Extrusions
14. Aachener Kolloquium Fahrzeug- und Motorentechnik, Aachen, 2005

[WHE02]   WHEELER, M.
Crashworthiness Of Aluminium Structured Vehicles
Alcan International, 2002

[WOH05]   WOHLECKER, W. / ICKERT, L.
Aluminium or steel? – Lightweight design in a vehicle hood
Forschungsgesellschaft Kraftfahrwesen mbH, Aachen
Euromotor Body, Aachen, 2005

[WHI06]   WHITE, M.
The new Jaguar XK car body – Car Body development and production
Jaguar & Land Rover, GB
The Consistent Lightweight Automobile 2006, Bad Nauheim, 2006